Elliptic Curves as Attractors in $\mathbb{P}^2$ Part 1: Dynamics

Araceli Bonifant, Marius Dabija, and John Milnor

CONTENTS

We study rational maps of the real or complex projective plane of degree two or more, concentrating on those that map a genus-one curve onto itself, necessarily by an expanding map. We describe relatively simple examples with a rich variety of interesting dynamical behaviors that are perhaps familiar to the applied dynamics community but not to specialists in several complex variables. For example, we describe smooth attractors with riddled or intermingled attracting basins, and we observe "blowout" bifurcations when the transverse Lyapunov exponent for the invariant curve changes sign. In the complex case, we prove that the genus-one curve (a topological torus) can never have a trapping neighborhood, yet it can have an attracting basin of large measure (perhaps even of full measure). We also describe examples in which there appear to be attracting Herman rings (topological cylinders mapped to themselves with irrational rotation number) with open attracting basin. Section 8 provides a more general discussion of Herman rings and Siegel disks for arbitrary holomorphic maps of $\mathbb{P}^2(\mathbb{C})$, and the last section outlines open problems.

1. INTRODUCTION

In [Bonifant and Dabija 02], the authors constructed many examples of rational maps f of the real or complex projective plane of degree $d \geq 2$ with a curve $\mathcal{C} = f(\mathcal{C})$ of genus one as invariant subset. In most of the examples, these rational maps are *holomorphic* (that is, everywhere defined). We will make some use of general rational maps that are allowed to have finitely many points of indeterminacy, but will usually concentrate on holomorphic maps. The case of a curve of genus one is of particular interest, since examples of holomorphic or rational self-maps with an invariant curve of genus zero are easy to construct, while higher-genus examples cannot exist. (See Remarks 1.5 and 2.2. Here the "genus" of a real curve is defined to be the genus of its complexification.) We will be primarily concerned with the case in which

2000 AMS Subject Classification: 37C70, 37F10, 37F45, 37F50

Keywords: Attractors, elliptic curves, Herman rings, intermingled basins, transverse Lyapunov exponent

1058-6458/2007 $0.50 per page

the invariant genus-one curve $\mathcal{C}$ is nonsingular, necessarily of degree three. In this case we refer to $\mathcal{C}$ as an *elliptic curve*.

The first seven sections of the present paper study the extent to which such an invariant genus-one curve $\mathcal{C} \subset \mathbb{P}^2$ can be an "attractor." We must distinguish several possible degrees of attraction.

Definition 1.1. Let $A = f(A)$ be a compact subset of $\mathbb{P}^2(\mathbb{C})$ or $\mathbb{P}^2(\mathbb{R})$.

1. A will be called a *measure-theoretic attractor* if it satisfies the following two conditions:
   (a) A is a *minimal-measure attracting set*, that is, its attracting basin (the union of all orbits that converge to A) has positive measure, but no closed proper subset has a basin of positive measure.[1]
   (b) It contains a *dense orbit*, and hence cannot be expressed as the union of strictly smaller closed invariant sets.
2. A will be called a *trapped attractor* if it satisfies the following two conditions:
   (a) A has a compact *trapping neighborhood* N such that $f(N) \subset N$ and $A = \bigcap_n f^{\circ n}(N)$.
   (b) A contains a dense orbit. (This property is again required to ensure indecomposability.)
3. A will be called a *global attractor* if it is a measure-theoretic attractor with the property that its attracting basin has full measure in the ambient space $\mathbb{P}^2$.

In both the real and complex cases, we provide examples in which an elliptic curve $\mathcal{C}$ is a measure-theoretic attractor. In fact, there are examples in which there are two distinct smooth algebraic curves that are measure-theoretic attractors and whose attracting basins are thoroughly intermingled, so that they have the same topological closure. We provide an example of a singular real genus-one quartic that is a trapped attractor, but we prove that a complex genus-one curve can never be a trapped attractor. In fact, it seems likely that the attracting basin of a complex genus-one curve cannot have interior points, so that the set of points that are *not* attracted to $\mathcal{C}$ must be everywhere dense. (Compare Lemma 4.5, as well as Proposition 6.4.)

We describe examples in which it seems possible that the genus-one curve is a global attractor, with attracting basin of full measure. We also provide a family of examples in which there appears to be a pair of Herman rings as attractor, with an open neighborhood as attracting basin.

Definition 1.2. By a *Herman ring* for a rational map f of $\mathbb{P}^2(\mathbb{C})$ we mean a complex one-dimensional annulus H that is holomorphically embedded in $\mathbb{P}^2(\mathbb{C})$ and that maps to itself by an irrational rotation under f or under some iterate of f. Similarly, a *Siegel disk* will mean a holomorphically embedded complex one-dimensional open disk that maps to itself by an irrational rotation under f or $f^{\circ k}$. Such a ring or disk is *maximal* if it cannot be embedded in a larger Herman ring or Siegel disk. (However, we will usually not assume maximality.) We will be particularly interested in the case in which all or part of such a ring or disk is transversally attracting. (See Section 8.)

1.1 An Outline of the Following Sections

Section 2 describes some basic ideas: the *transverse Lyapunov exponent* along an invariant genus-one curve is a primary indicator of whether the curve is attracting. Methods for actually computing this transverse exponent will be described in Part 2, the sequel to this paper; however, the conclusions of these computations are often quoted below. Section 3 describes the very restrictive class of rational maps with a first integral. These are used in Section 4 to construct a three-parameter family of more-interesting rational maps of degree four.

Section 5 studies eight explicit examples, with conjectured descriptions based on numerical computation. In the first three examples, randomly chosen orbits always seem to converge to the Fermat curve $x^3 + y^3 + z^3 = 0$, both in the real case with ambient space $\mathbb{P}^2(\mathbb{R})$ and in the complex case with ambient space $\mathbb{P}^2(\mathbb{C})$. This suggests that the real or complex Fermat curve may be a global attractor, with attracting basin of full measure. (However, such experiments can never be decisive, since other attractors with basins of extremely small measure could easily be missed by our random samples.) Example 5.5 suggests that a cycle of two Herman rings can be a measure-theoretic attractor in $\mathbb{P}^2(\mathbb{C})$ (perhaps even a

[1] See [Milnor 85], and compare the discussion of "Milnor attractors" in [Kaneko 02, Kaneko 03] or [Ashwin et al. 96]. For other concepts of attractor, see Remark 5.8, as well as [Auslander et al. 64]. For interesting examples in the real case see [Alexander et al. 92, Kan 94, Maistrenko et al. 98, Ashwin et al. 96, Ott and Sommerer 94, Ott et al. 93]; and for attractors in $\mathbb{P}^2(\mathbb{C})$, see [Fornæss and Sibony 01, Fornæss and Weickert 99, Jonsson and Weickert 00].

global attractor) for such a map with invariant genus-one curve. In Example 5.6, there is an attracting fixed point at the "north pole," while the "equator" is an invariant $\mathbb{P}^1$ that forms a measure-theoretic attractor. In Example 5.7 a typical orbit seems to spend most of its time bouncing between the three coordinate axes, but sometimes escaping briefly. This section concludes with examples of lower-degree maps that have an invariant elliptic curve. In particular, Example 5.10 describes a degree-3 map of $\mathbb{P}^2(\mathbb{C})$ that appears to have the Fermat curve as a global attractor.

All of these conclusions are empirical, based on numerical computation. However, Sections 6 and 7 provide cases with explicit proofs. Example 6.2 considers *elementary maps*, which carry each line through a preferred point ϱ_0 to a line through ϱ_0. It describes examples that have three different attractors with thoroughly intermingled basins, all of positive measure. (See [Alexander et al. 92] for similar examples.) Two of these basins are dense in the Julia set, while the third basin, which is everywhere dense, is equal to the Fatou set. Note that we use these terms with their classical meanings:

Definition 1.3. The *Fatou set* is defined to be the largest open set on which the sequence of iterates of f forms a normal family; and the *Julia set*[2] J is defined to be its complement in $\mathbb{P}^2(\mathbb{C})$.

Theorem 7.2 provides examples of singular real quartic curves of genus one that are trapped attractors under suitable rational maps, while Theorem 7.4 shows that a complex genus-one curve can never be a trapped attractor. (We don't know whether nonsingular real curves can be trapped attractors.) Section 8 provides a more general discussion of Herman rings. The transverse Lyapunov exponent for a (complex one-dimensional) Herman ring or Siegel disk in $\mathbb{P}^2(\mathbb{C})$ provides a strict criterion for attraction or repulsion. This exponent is no longer constant, as it was in the case of a genus-one curve, but is rather a convex piecewise linear function on the ring or disk, constant on each invariant circle. We prove the persistence of invariant circles in $\mathbb{P}^2(\mathbb{R})$ under suitable hypotheses, but our results are not strong enough to prove the conjecture that the associated Herman rings in $\mathbb{P}^2(\mathbb{C})$ are also persistent. Section 9 concludes the discussion by providing a brief outline of open problems.

We will usually concentrate on the complex case, although many of the figures will necessarily illustrate the real case.

Remark 1.4. (Computation.) Numerical computations are extremely delicate near the invariant curve $\mathcal{C}$. Thus it is essential to work with multiple-precision arithmetic; even so, numerical simulation of the dynamics must be understood as a hint of the true state of affairs, rather than a definitive answer. One surprising aspect of these maps is that in some cases orbits tend to spend quite a bit of time *extremely* close to $\mathcal{C}$ even when the transverse exponent is positive. (Compare Figures 5 and 10.) In a similar situation, in [Maistrenko et al. 98, p. 2713], the authors report that in the presence of a small positive value of the transverse exponent,

> ... a trajectory may spend a very long time in the neighborhood of the invariant subspace. From time to time, the repulsive character of the chaotic set manifests itself, and the trajectory exhibits a burst in which it moves far away from the invariant subspace, to be reinjected again into the proximity of this subspace.... [The] positive value of the Lyapunov exponent applies over long periods of time. For shorter time intervals, the net contribution... may be negative, and the trajectory is attracted to the chaotic set.

(Similar behavior was described in [Platt et al. 93].)

Remark 1.5. (Genus zero.) Some examples of holomorphic self-maps of $\mathbb{P}^2$ with attracting invariant curves of genus zero are easy to construct. Thus, for the map

$$(x : y : z) \mapsto (x : y : z/2),$$

the line $z = 0$ is an attracting curve with the region $|z|^2 < |x|^2 + |y|^2$ as trapping neighborhood. Similarly, if $(x : y) \mapsto (f_1(x, y) : f_2(x, y))$ is any rational map of $\mathbb{P}^1$ of degree $d \geq 2$, then the line $z = 0$ is a trapped attracting curve for the map $(x : y : z) \mapsto (f_1(x, y) : f_2(x, y) : z^d)$. In particular, if we start with a map of $\mathbb{P}^1$ that has a dense orbit (for example, a Lattès map; compare Remark 4.8), then we obtain a trapped attractor. (See also Example 8.1.)

[2]Caution: Other possible definitions of Julia set are sometimes used in the literature. Compare [Fornæss and Sibony 94, Fornæss and Sibony 95b, Fornæss and Sibony 95a, Hubbard and Papadopol 94, Sibony 99], and see [Briend and Duval 01, Briend and Duval 99, Guedj 05] for related results.

2. RATIONAL MAPS AND THE TRANSVERSE LYAPUNOV EXPONENT

Let f be a rational map of $\mathbb{P}^2 = \mathbb{P}^2(\mathbb{C})$. We can write $f : \mathbb{P}^2 \smallsetminus \mathcal{I}_f \to \mathbb{P}^2$, where

$$f(x : y : z) = \big(f_1(x, y, z) : f_2(x, y, z) : f_3(x, y, z)\big),$$

using homogeneous coordinates $(x : y : z)$ (representing a point $(x, y, z) \in \mathbb{C}^3 \smallsetminus \{(0, 0, 0)\}$, which is well defined only up to multiplication by a nonzero constant). Here f_1, f_2, f_3 are to be homogeneous polynomials of the same degree $d = \deg(f) \geq 2$ with no common factor, and $\mathcal{I}_f$, the *indeterminacy set*, is the finite set consisting of all common zeros of f_1, f_2, f_3. By definition, d is the *algebraic degree* of f. Such a rational map f is called *holomorphic* if $\mathcal{I}_f$ is vacuous, so that f is an everywhere-defined map from $\mathbb{P}^2$ to itself. The topological degree of f as a map from $\mathbb{P}^2$ to itself is then equal to d^2, while the algebraic number of fixed points is $d^2 + d + 1$. However, if $\mathcal{I}_f \neq \varnothing$, then there will be fewer fixed points (or sometimes an entire curve of fixed points), and a generic point will have fewer than d^2 preimages.

Now consider an algebraic curve $\mathcal{C} \subset \mathbb{P}^2$, defined by a homogeneous equation $\Phi(x, y, z) = 0$, with degree $\deg(\mathcal{C}) = \deg(\Phi) \geq 1$. We will say that a *rational map* f is *well defined* on $\mathcal{C}$ if the intersection $\mathcal{C} \cap \mathcal{I}_f$ is empty, so that f is defined and holomorphic throughout a neighborhood of $\mathcal{C}$. It then follows that the image $\mathcal{C}' = f(\mathcal{C})$ is itself an algebraic curve with $\deg(\mathcal{C}') \geq 1$. Furthermore, the degree of the restriction $f|_{\mathcal{C}} : \mathcal{C} \to \mathcal{C}'$ is determined by the relation[3]

$$\deg(f)\deg(\mathcal{C}) = \deg(f|_{\mathcal{C}})\deg(\mathcal{C}'). \tag{2–1}$$

Definition 2.1. An algebraic curve $\mathcal{C} \subset \mathbb{P}^2$ will be called *invariant* under f if f is well defined on $\mathcal{C}$ and if $f(\mathcal{C}) = \mathcal{C}$. It then follows from (2–1) that the degree of the restriction $f|_{\mathcal{C}} : \mathcal{C} \to \mathcal{C}$ is precisely equal to $\deg(f)$, the degree of the equations that define f.

On the other hand, if $\mathcal{C}$ contains points of indeterminacy, then these remarks break down. For example, $\mathcal{C} \smallsetminus (\mathcal{I}_f \cap \mathcal{C})$ may consist entirely of fixed points, or may map to a single point under f. In the case that $\mathcal{I}_f \cap \mathcal{C}$ is nonempty but the image $f\big(\mathcal{C} \smallsetminus (\mathcal{I}_f \cap \mathcal{C})\big)$ is contained in $\mathcal{C}$, the curve $\mathcal{C}$ will be called *weakly f-invariant*. If $\mathcal{C}$ is smooth and weakly invariant, then f extends uniquely to a holomorphic map from $\mathcal{C}$ to itself; but the degree on $\mathcal{C}$ may be smaller than $\deg(f)$. (Compare Remarks 4.2 and 6.9 below.)

Remark 2.2. (Curves of higher genus.) As one consequence of this discussion, it follows that a curve of genus $g \geq 2$ can never be invariant under a map of $\mathbb{P}^2$ of degree $d \geq 2$. For it follows from the Riemann–Hurwitz formula (see, for example, [Milnor 06b]) that a curve of genus ≥ 2 does not admit any self-maps of degree ≥ 2.

Returning to the genus-one case, let $\mathcal{D}(n) = n\,\mathcal{D}(1)$ be the divisor class on $\mathcal{C}$ obtained by intersecting $\mathcal{C}$ with a generic curve of degree n in $\mathbb{P}^2$. A given holomorphic map $g : \mathcal{C} \to \mathcal{C}$ of degree $d > 0$ extends to a rational map of $\mathbb{P}^2$ that is well defined on $\mathcal{C}$ if and only if

$$g^*\mathcal{D}(1) = \mathcal{D}(d).$$

(See [Bonifant and Dabija 02, Section 2]. For a more general result see [Fakhruddin 03].)

If $d < \deg(\mathcal{C})$, then this extension is unique; but if $d \geq \deg(\mathcal{C})$, then there exists a $3\binom{d-\deg(\mathcal{C})+2}{2}$-dimensional family of such extensions, since we can always replace the associated homogeneous polynomial map $F : \mathbb{C}^3 \to \mathbb{C}^3$ by $F + \Phi H$, where $\Phi = 0$ is the defining equation for $\mathcal{C}$, and where $H : \mathbb{C}^3 \to \mathbb{C}^3$ is any homogeneous map with $\deg(H) = d - \deg(\mathcal{C})$. In this case, a *generic* extension will be holomorphic (i.e., defined everywhere).

Any compact Riemann surface of genus one is conformally isomorphic to some elliptic curve in $\mathbb{P}^2$, which is uniquely determined up to a conformal automorphism of $\mathbb{P}^2$. (Compare [Griffiths and Harris 94, p. 222].) Alternatively, it is conformally isomorphic to some flat torus $\mathbb{C}/\Omega$, where Ω is a lattice that is uniquely determined up to multiplication by a constant.

One particular virtue of curves of genus one is that the holomorphic self-maps are very well understood. For any genus-one curve $\mathcal{C} \subset \mathbb{P}^2$ there is a holomorphic immersion

$$\upsilon : \mathbb{C}/\Omega \to \mathcal{C}$$

that is one-to-one except over finitely many singular points in the case of a singular curve (with degree greater than three) and is biholomorphic in the case of an elliptic curve (of degree three). Any holomorphic self-map of $\mathcal{C}$ lifts to a holomorphic self-map of $\mathbb{C}/\Omega$, which is necessarily affine, $t \mapsto at + b$.

It follows easily that the normalized Lebesgue measure on $\mathbb{C}/\Omega$ pushes forward to a canonical smooth probability

[3] Proof outline: A generic line L intersects $\mathcal{C}'$ in $\deg(\mathcal{C}')$ distinct points, none of which is a critical value of $f|_{\mathcal{C}}$. Each of these has $\deg(f|_{\mathcal{C}})$ preimages in $\mathcal{C}$. On the other hand, by Bézout's theorem, the curve $f^{-1}(L)$ of degree $\deg(f)$ will intersect $\mathcal{C}$ in $\deg(f)\deg(\mathcal{C})$ points, counted with multiplicity. In fact, for generic L, each of these intersections will be transverse, and it follows that $\deg(f)\deg(\mathcal{C}) = \deg(f|_{\mathcal{C}})\deg(\mathcal{C}')$, as required.

measure λ on $\mathcal{C}$ that is invariant under every nonconstant self-map. The derivative a of the affine map on $\mathbb{C}/\Omega$ will be called the *multiplier* of f on $\mathcal{C}$. Note that the product $a\Omega$ is a sublattice of finite index in Ω, and that $|a|^2$ is equal to the index of this sublattice. Equivalently, $|a|^2$ is the topological degree of f considered as a map from $\mathcal{C}$ to itself. In particular, $|a|^2$ is equal to the algebraic degree d of f whenever $\mathcal{C} \subset \mathbb{P}^2$ is invariant under the rational map f. Since we always assume that $d \geq 2$, it follows that this canonical measure λ is ergodic.

In the case of a genus-one curve defined by equations with real coefficients, the real curve

$$\mathcal{C}(\mathbb{R}) = \mathcal{C} \cap \mathbb{P}^2(\mathbb{R})$$

has at most two connected components. If $\mathcal{C}(\mathbb{R})$ is mapped into itself by a rational map f of $\mathbb{P}^2(\mathbb{R})$, then at least one connected component, say $\mathcal{C}^0(\mathbb{R})$, must map onto itself under f or under $f \circ f$. In this case we have a uniformizing map $\mathbb{R}/\mathbb{Z} \to \mathcal{C}^0(\mathbb{R})$ such that f (or $f \circ f$) corresponds to a map on $\mathbb{R}/\mathbb{Z}$ that is linear with constant integer multiplier. Such an invariant component $\mathcal{C}^0(\mathbb{R})$ has a canonical invariant probability measure.

2.1 The Transverse Lyapunov Exponent

Let $\mathcal{C}$ be an elliptic curve, invariant under the rational map f. We will describe an associated real number that is conjectured to be negative if and only if $\mathcal{C}$ is a measure-theoretic attractor. To fix ideas we will concentrate on the complex case, but constructions in the real case are completely analogous. The notation $T\mathbb{P}^2|_{\mathcal{C}}$ will be used for the complex 2-plane bundle of vectors tangent to $\mathbb{P}^2(\mathbb{C})$ at points of the submanifold $\mathcal{C}$, and the abbreviated notation $T_{\pitchfork}\mathcal{C}$ will be used for the "transverse" complex line bundle over $\mathcal{C}$ having the quotient vector space

$$T_{\pitchfork}(\mathcal{C}, p) = T(\mathbb{P}^2, p)/T(\mathcal{C}, p)$$

as typical fiber. In other words, there is a short exact sequence $0 \to T\mathcal{C} \to T\mathbb{P}^2|_{\mathcal{C}} \to T_{\pitchfork}\mathcal{C} \to 0$ of complex vector bundles over $\mathcal{C}$.

It is sometimes convenient to refer to $T_{\pitchfork}\mathcal{C}$ as the "*normal bundle*" of $\mathcal{C}$, although that designation isn't strictly correct. If $f : \mathbb{P}^2 \to \mathbb{P}^2$ with $f(\mathcal{C}) \subset \mathcal{C}$, then f induces linear maps

$$f'_{\pitchfork}(p) : T_{\pitchfork}(\mathcal{C}, p) \to T_{\pitchfork}(\mathcal{C}, f(p)), \qquad (2\text{–}2)$$

and these linear maps collectively form a fiberwise linear self-map $f'_{\pitchfork} : T_{\pitchfork}\mathcal{C} \to T_{\pitchfork}\mathcal{C}$.

Now choose a metric on this complex normal bundle. That is, choose a norm $\|\vec{v}\,\|_{\pitchfork}$ on each quotient vector space $T_{\pitchfork}\mathcal{C}$ that depends continuously on $\vec{v}$, vanishes only on zero vectors, and satisfies $\|t\vec{v}\,\|_{\pitchfork} = |t|\|\vec{v}\,\|_{\pitchfork}$. Then the linear map $f'_{\pitchfork}$ of (2–2) has an operator norm

$$\|f'_{\pitchfork}(p)\| = \|f'_{\pitchfork}\vec{v}\,\|_{\pitchfork}/\|\vec{v}\,\|_{\pitchfork},$$

which is well defined and satisfies the chain rule. Here $\vec{v}$ can be any nonzero vector in the fiber $T_{\pitchfork}(\mathcal{C}, p)$ over p. By definition, the *transverse Lyapunov exponent* along the invariant elliptic curve $\mathcal{C}$ is equal to the rate of exponential growth

$$\mathrm{Lyap}_{\mathcal{C}} = \lim_{k\to\infty} (1/k) \log \|(f^{\circ k})'_{\pitchfork}(p)\|$$

for almost every choice of initial point $p \in \mathcal{C}$. By the Birkhoff ergodic theorem, this coincides with the average value

$$\mathrm{Lyap}_{\mathcal{C}}(f) = \int_{\mathcal{C}} \log \|f'_{\pitchfork}(p)\| d\lambda(p).$$

Using the fact that the measure λ is invariant under f, it is not hard to check directly that this average value is independent of the choice of metric.

Thus a *negative value* of $\mathrm{Lyap}_{\mathcal{C}}$ means that under iteration of f, almost any point that is "infinitesimally close" to $\mathcal{C}$ will converge to $\mathcal{C}$. A key role in this case is played by the stable sets of the various points $p \in \mathcal{C}$. By definition, the *stable set* of p is the union of all connected sets containing p for which the diameter of the nth forward image tends to zero as n tends to ∞.

Many such stable sets are smooth curves. With a little imagination, some of these are clearly visible in Figures 3–6, 10, 11, 13, and 14. It is natural to expect that negative values of $\mathrm{Lyap}_{\mathcal{C}}$ will imply that $\mathcal{C}$ is a measure-theoretic attractor.[4] On the other hand, if $\mathrm{Lyap}_{\mathcal{C}} > 0$, then almost any "infinitesimally close" point will be pushed away from $\mathcal{C}$. It seems natural to conjecture that positive values of $\mathrm{Lyap}_{\mathcal{C}}$ should imply that the attracting basin of $\mathcal{C}$ has measure zero. However, this seems like a difficult question. (Compare Remark 6.8.) The term *blowout bifurcation* has been introduced in [Ott and Sommerer 94] for a transition in which a transverse Lyapunov exponent crosses through zero. (Compare [Maistrenko et al. 98] or [Ashwin et al. 98].)

[4] A sketch of a proof is given in [Alexander et al. 92], using a version of Pesin theory to construct stable manifolds. However, the details are difficult because of the presence of varieties of critical points for our maps. We will not try to provide a proof in this paper, except in one very special case (Theorem 6.3 below).

3. MAPS WITH FIRST INTEGRAL

By definition, a *first integral* for a dynamical system is a nonconstant function that is constant on each orbit. In particular, by a *first integral* for a rational map $f : \mathbb{P}^2 \smallsetminus \mathcal{I}_f \to \mathbb{P}^2$ we will mean a nonconstant rational function $\eta : \mathbb{P}^2 \smallsetminus \mathcal{I}_\eta \to \mathbb{P}^1$ with values in the projective line that satisfies

$$\eta\big(f(x : y : z)\big) = \eta(x : y : z)$$

whenever both sides are defined. Identifying $\mathbb{P}^1$ with the Riemann sphere $\widehat{\mathbb{C}} = \mathbb{C} \cup \{\infty\}$, we can write

$$\eta(x : y : z) = \Phi(x, y, z)/\Psi(x, y, z) \in \widehat{\mathbb{C}},$$

where Φ and Ψ are homogeneous polynomials of the same degree without common factor. Equivalently, the loci $\{\eta = \text{constant}\}$ form a pencil of algebraic curves

$$\alpha\,\Phi(x, y, z) + \beta\,\Psi(x, y, z) = 0 \tag{3–1}$$

that are weakly invariant under f (Definition 2.1). Intuitively, these weakly invariant curves yield a somewhat singular "foliation" of the projective plane. The curves in this pencil intersect only in the finite set $\mathcal{I}_\eta$ consisting of common zeros of Φ and Ψ. (Note that a point can be contained in two such weakly invariant curves only if it is either periodic or a point of indeterminacy for f.) We will be interested in maps with a pencil of weakly invariant elliptic curves. Such maps are exceedingly special. For example, we have the following lemma.

Lemma 3.1. (Maps with first integral.) *Let f be a rational map with first integral such that a generic point of $\mathbb{P}^2$ is contained in an elliptic curve that is mapped to itself with degree $d \geq 2$. Then:*

(i) *There are no dense orbits, since every orbit is contained in a weakly invariant curve.*

(ii) *Periodic points, repelling along this curve, are everywhere dense. Hence the Fatou set is empty.*

(iii) *For most values of n there are infinitely many fixed points of $f^{\circ n}$, with at least one in each weakly invariant curve. Hence there must be an entire algebraic curve of such points.*

(iv) *The indeterminacy set $\mathcal{I}_f$ is necessarily nonempty (even after a finite number of blowups of $\mathbb{P}^2(\mathbb{C})$).*

Proof: The last statement follows because there are infinitely many points of fixed period n. (Note also that a generic point has only d preimages, all lying in the weakly invariant curve that passes through it, rather than the d^2 preimages it would have in the holomorphic case.) The other statements are easily verified. □

Here is a class of examples that generalize a construction due to A. Desboves in 1886 (see [Desboves 86]). For any smooth cubic curve $\mathcal{C} \subset \mathbb{P}^2$, there is a canonical map $f : \mathcal{C} \to \mathcal{C}$ called the *tangent process*, constructed as follows. For any point $p \in \mathcal{C}$, let $L_p \subset \mathbb{P}^2$ be the unique line tangent to $\mathcal{C}$ at p. Then the image $f(p)$ is defined by the equation

$$L_p \cap \mathcal{C} = \{p\} \cup \{f(p)\}.$$

This is closely related to the standard additive group law on $\mathcal{C}$. In fact, if we choose the parametrization $\upsilon : \mathbb{C}/\Omega \to \mathcal{C}$ of Section 2, so that $\upsilon(0)$ is one of the nine flex points of $\mathcal{C}$, then three distinct points t_j of $\mathbb{C}/\Omega$ will have sum $t_1 + t_2 + t_3$ equal to zero if and only if the images $\upsilon(t_j) \in \mathcal{C}$ are collinear. In our case, since there is a double intersection at p, we obtain the equation $2t_1 + t_3 = 0$ or $t_1 \mapsto t_3 = -2t_1$. Thus f has multiplier -2 and degree 4.

Now start with two distinct cubic curves in $\mathbb{P}^2$, described by homogeneous equations $\Phi(x, y, z) = 0$ and $\Psi(x, y, z) = 0$. Then there is an entire one-parameter family of such curves, given by (3–1), that fill out the projective plane. In fact, any point of $\mathbb{P}^2$ that is not a common zero of Φ and Ψ belongs to a unique curve

$$\Phi/\Psi = \text{constant} = -\beta/\alpha \in \widehat{\mathbb{C}}.$$

If a generic curve in our one-parameter family is smooth, then a generic point $p \in \mathbb{P}^2$ belongs to a unique smooth curve $\mathcal{C}_p$ in the family. Applying the tangent process at p, we obtain a well-defined image point $f(p) \in \mathcal{C}_p$. Since p is generic, this extends to a uniquely defined rational map of $\mathbb{P}^2$ that carries each curve of our family into itself.

Let us specialize to the classical example given by O. Hesse in 1884 (see [Hesse 44]), with $\Phi(x, y, z) = x^3 + y^3 + z^3$ and $\Psi(x, y, z) = 3xyz$. (Compare [Artebani and Dolgachev 06]. Here the factor 3 has been inserted for later convenience.) The corresponding foliation of the real projective plane $\mathbb{P}^2(\mathbb{R})$ by the curves of (3–1) is illustrated in Figure 1. This foliation has three kinds of singularities, all clearly visible in the figure:

(a) There are three singularities for which two of the three coordinates x, y, z are zero. These all lie in the real plane $\mathbb{P}^2(\mathbb{R}) \subset \mathbb{P}^2(\mathbb{C})$.

(b) There are three singularities in the real plane (or nine in the complex plane) for which *all* of these curves

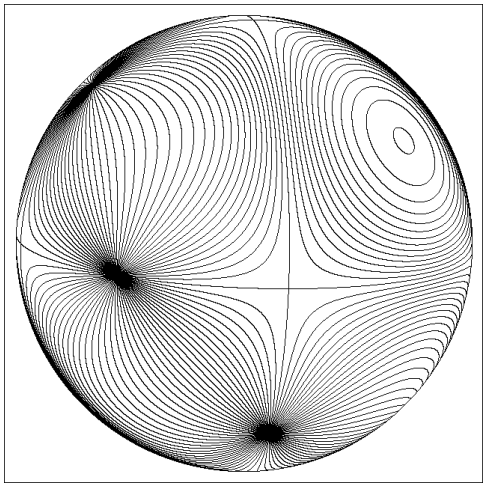

FIGURE 1. Hesse "foliation" of the real projective plane by the pencil of elliptic curves $\Phi/\Psi = \kappa \in \widehat{\mathbb{C}}$, where $\Phi = x^3 + y^3 + z^3$ and $\Psi = 3xyz$. Here $\mathbb{P}^2(\mathbb{R})$ is represented as a unit 2-sphere with antipodal points identified. These real curves intersect only at their three common inflection points, which look dark in the figure. In the limiting case as $\kappa \to \infty$, the curve $\Phi = \kappa\Psi$ degenerates to the union $xyz = 0$ of the three coordinate lines, which intersect at the points $(-1, 0, 0)$, $(0, 1, 0)$, and $(0, 0, 1)$ respectively near the left, top, and center of the figure.

intersect at common flex points. Each of these lies along just one of the three coordinate axes.

(c) There is one real singularity (or nine complex singularities) for which $x^3 = y^3 = z^3$, represented by the center in the upper right of Figure 1.

According to Desboves, the tangent processes for these various curves $\Phi/\Psi = \kappa$ fit together to yield a well-defined rational map $f_0 : \mathbb{P}^2 \smallsetminus \mathcal{I}_{f_0} \to \mathbb{P}^2$ given by the formula

$$f_0(x : y : z) = \big(x(y^3 - z^3) : y(z^3 - x^3) : z(x^3 - y^3)\big). \tag{3–2}$$

The indeterminacy set $\mathcal{I}_{f_0}$ for this *classical Desboves map* consists of the twelve points of types (a) and (c), as listed above. This particular example has the advantage (as compared with an arbitrary choice for Φ and Ψ) that most of the curves in our one-parameter family are non-singular and contain no points of indeterminacy. The only exceptions are the curves $\Phi = \kappa\Psi$ with $\kappa^3 = 1$, which are singular at points of indeterminacy of type (c), and the degenerate case $\Psi = 0$ (corresponding to $\kappa = \infty \in \widehat{\mathbb{C}}$) with singular indeterminacy points of type (a). The foliation singularities of type (b), where all of the curves intersect, are all fixed points at which the value $f_0(p) = p$ is well defined.

For further examples of rational maps of $\mathbb{P}^2$ with first integral, see Example 5.10 and Remark 6.9.

4. THE DESBOVES FAMILY

Let $\Phi(x, y, z)$ be the homogeneous polynomial $x^3 + y^3 + z^3$. The *Fermat curve* $\mathcal{F}$ is defined as the locus of zeros $\Phi(x, y, z) = 0$ in the projective plane $\mathbb{P}^2$. (Here we can work either over the real numbers or over the complex numbers.) Most of the examples in Section 5 will belong to a family of fourth-degree rational maps of $\mathbb{P}^2$ that carry this Fermat curve into itself, as introduced in [Bonifant and Dabija 02, Section 6.3]. We will call these *Desboves maps*, since they arise from a simple perturbation of the classical Desboves map f_0 of (3–2). Evidently f_0 lifts to a homogeneous polynomial map

$$F_0(x, y, z) = \Big(x(y^3 - z^3)\,, y(z^3 - x^3)\,, z(x^3 - y^3)\Big)$$

from $\mathbb{C}^3$ to itself. Geometrically, f_0 is defined by the property that the line from p to $f_0(p)$ is tangent to the elliptic curve $(x^3+y^3+z^3)/3xyz = \kappa$, which passes through the point p. Its set of fixed points on each smooth curve in our family coincides with the intersection

$$x^3 + y^3 + z^3 = 3xyz = 0,$$

and can also be identified with the set of points of inflection on any one of these curves, or as the set of points where all of these curves intersect. This map f_0 is not everywhere defined: it has a twelve-point set of points of indeterminacy as described at the end of Section 3. However, for any specified curve $\Phi_\kappa(x, y, z) = x^3 + y^3 + z^3 - 3\kappa xyz = 0$ in our family, if we replace F_0 by the sum

$$F_L(x, y, z) = F_0(x, y, z) \,+\, L(x, y, z)\,\Phi_\kappa(x, y, z),$$

where L is any linear map from $\mathbb{C}^3$ to itself, then we obtain a new map f_L of $\mathbb{P}^2(\mathbb{C})$ that coincides with f_0 on the particular curve $\Phi_\kappa(x, y, z) = 0$. For a generic choice of L, the resulting map f_L of $\mathbb{P}^2(\mathbb{C})$ is well defined everywhere.

To simplify the discussion, we will restrict attention to the case $\kappa = 0$, taking

$$\Phi(x, y, z) = \Phi_0(x, y, z) = x^3 + y^3 + z^3,$$

and we will take a linear map L that is described by a diagonal matrix,

$$L(x, y, z) = (ax, by, cz).$$

Definition 4.1. (Desboves maps.) The resulting 3-parameter family of maps of the real or complex projective plane will be called the family of *Desboves maps*. These maps $f = f_{a,b,c}$ are given by the formula

$$f(x:y:z) = \Big(x(y^3 - z^3 + a\Phi) : y(z^3 - x^3 + b\Phi) : z(x^3 - y^3 + c\Phi)\Big), \tag{4–1}$$

where a, b, c are the parameters. Each such f maps the Fermat curve $\mathcal{F}$, defined by the equation $\Phi(x, y, z) = 0$, into itself. Furthermore, each f maps each of the coordinate lines $x = 0$, $y = 0$, $z = 0$ into itself.

For special values of the parameters, the map f may have points of indeterminacy (but never on the curve). However, for a generic choice of parameters, f is everywhere defined. More explicitly, it is not hard to see that f is an everywhere-defined holomorphic map from $\mathbb{P}^2$ to itself if and only if we avoid a union of seven hyperplanes in the space $\mathbb{C}^3$ of parameters, defined by the equation

$$abc(a + b + c)(a + 1 - b)(b + 1 - c)(c + 1 - a) = 0.$$

Remark 4.2. (Fixed points.) Generically, each complex Desboves map has 21 distinct fixed points (nine with $xyz \neq 0$, nine on the Fermat curve with just one of the coordinates equal to zero, and three with two of the coordinates equal to zero). However, there are two kinds of exception:

(i) If the product $abc\,(a + b + c)$ is zero, then one or more of the fixed points will be replaced by an indeterminacy point.

(ii) If one or more of the differences $b-a$, $c-b$, $a-c$, is equal to $+1$, then there is not only an indeterminacy point but also an entire line of fixed points.

In any case, there are exactly nine fixed points on the complex Fermat curve $\mathcal{F}$, forming the intersection of $\mathcal{F}$ with the locus $xyz = 0$. Consider, for example, the three points $(0 : \sqrt[3]{-1} : 1)$ obtained by intersecting the curve $\mathcal{F}$ with the invariant line $x = 0$. If we introduce the coordinate $Y = y/z \in \widehat{\mathbb{C}}$ on this line, then the restriction of the map f to this line is a rational map given by the formula

$$Y \mapsto Y\frac{b\,Y^3 + (b+1)}{(c-1)Y^3 + c}\,,$$

with fixed points at $Y = 0$, at $Y = \infty$, and at the three points $Y^3 = -1$. A brief computation shows that the derivatives of this one-variable map at these five fixed points are respectively

$$(b+1)/c, \quad (c-1)/b, \quad 3(c-b) - 2\,, \tag{4–2}$$

where the last, corresponding to intersections of $x = 0$ with the Fermat curve, is counted three times. (Something very exceptional occurs in the special case $c = b+1$: all five derivatives are $+1$, and in fact, *every* point on the line $x = 0$ is fixed under f.) Similarly, permuting the coordinates cyclically, we obtain corresponding formulas for the invariant lines $y = 0$ and $z = 0$.

Remark 4.3. (The attracting basin.) According to [Bonifant and Dabija 02, Theorem 5.4], if $\mathcal{C} = f(\mathcal{C})$ is any invariant elliptic curve, then the set of iterated preimages of any point of $\mathcal{C}$ is everywhere dense in the Julia set $J(f)$. (Observe that since $\mathcal{C}$ is elliptic, the set of preimages of any point of $\mathcal{C}$ is everywhere dense in $\mathcal{C}$. It follows easily that the closure of the set of all preimages of a point in $\mathcal{C}$ does not depend on which point we start with.)

It seems likely that the following further statement is true:

Conjecture 4.4. *The entire attracting basin $\mathcal{B}(\mathcal{C})$ of an invariant elliptic curve $\mathcal{C}$ consisting of all points whose forward orbits converge to $\mathcal{C}$ is contained in the Julia set $J(f)$. Since iterated preimages of points in $\mathcal{C}$ are certainly in $\mathcal{B}(\mathcal{C})$, this implies that the closure $\overline{\mathcal{B}(\mathcal{C})}$ is precisely equal to $J(f)$.*

An immediate consequence would be the following. (For a special case, see Proposition 6.4.)

Lemma 4.5. (No interior points?) *If Conjecture 4.4 is true, then for any rational map $f_{a,b,c}$ in the Desboves family, the attracting basin $\mathcal{B}(\mathcal{F})$ has no interior points. In other words, the complementary set $\mathbb{P}^2(\mathbb{C}) \smallsetminus \mathcal{B}(\mathcal{F})$, consisting of points that are* not *attracted to $\mathcal{F}$, is everywhere dense in $\mathbb{P}^2(\mathbb{C})$.*

Proof: We must show that every point of $\mathcal{B} = \mathcal{B}(\mathcal{F})$ can be approximated arbitrarily closely by points outside of $\mathcal{B}$. Assuming the conjecture, it suffices to prove that every point of the Julia set $J(f_{a,b,c})$ can be approximated by points outside of $\mathcal{B}$. Since the average of the differences $c - b$, $b - a$, and $a - c$ is zero, it follows from (4–2) that the average of the transverse derivatives at the fixed points of f in $\mathcal{F}$ is -2. Hence at least one of these fixed points is strictly repelling.

Suppose, for example, that the points $(0 : \sqrt[3]{-1} : 1)$ are repelling within the line $x = 0$. Then the intersection of the basin $\mathcal{B}$ with this line consists of only countably many iterated preimages of these points. Therefore there

are points $(0 : y : z)$ arbitrarily close to $(0 : -1 : 1)$ that are not in this basin. Since every point of $J(f_{a,b,c})$ can be approximated by iterated preimages of $(0 : -1 : 1)$, it can also be approximated by iterated preimages of such points $(0 : y : z)$, as required. □

On the other hand, some of these fixed points on $\mathcal{F}$ may be attracting in the transverse direction. For example, if $|3(c-b)-2| < 1$, then each of the three fixed points where $\mathcal{F}$ intersects the line $x = 0$ is a *saddle*, repelling along the Fermat curve, but attracting along this line, which intersects it transversally. The *stable manifold* for such a saddle point can be identified with its immediate attracting basin within the line $x = 0$. It is not hard to check that this stable manifold is contained in the Julia set. Hence its iterated preimages must be dense in the Julia set.

The attraction within this stable manifold will be particularly strong if $c-b = \frac{2}{3}$, so that the transverse derivative $3(c-b)-2$ is zero, or in other words, so that the associated fixed point is transversally superattracting. Similarly, the transverse derivative at the three points where $y = 0$ (or where $z = 0$) is zero if and only if $a-c = \frac{2}{3}$ (or respectively $b-a = \frac{2}{3}$).

Definition 4.6. (The two-thirds family.) We will say that f belongs to the *two-thirds family* if two of the three differences $b-a$, $c-b$, and $a-c$ are equal to $\frac{2}{3}$, or equivalently, if two-thirds of the fixed points on the Fermat curve are transversally superattracting. (There are nine such fixed points in the complex case and three in the real case.) The average of the values of the transverse derivative at these fixed points is always -2, so if two out of the three values are zero, then it follows that the remaining value is -6, rather strongly repelling. To fix ideas, let us suppose that

$$(a, b, c) = \left(b - \frac{2}{3},\ b,\ b + \frac{2}{3}\right),$$

so that the transverse derivative is zero when $x = 0$ or $z = 0$, and -6 when $y = 0$. The associated transverse Lyapunov exponent, plotted as a function of b, is shown in Figure 2. In the real case, this transverse exponent is negative (that is, attracting) if and only if $|b| < 0.901\ldots$, while in the complex case it is negative if and only if $b < 0.274\ldots$. See Part 2 of this paper for such computations. (It seems empirically that the real Fermat curve is strictly "more attracting" than the corresponding complex Fermat curve except in a few isolated cases. However, we do not have any explanation for this phenomenon.)

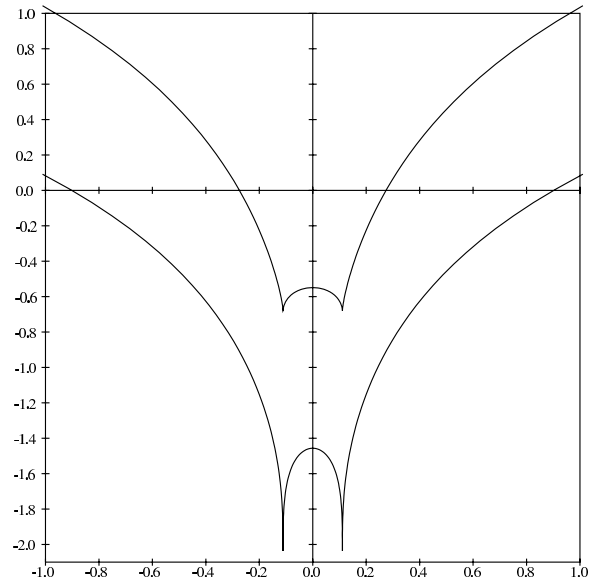

FIGURE 2. Graph of the transverse exponents along the real and complex Fermat curves as functions of the middle parameter b for the "two-thirds family" of Definition 4.6, with Desboves parameters $\left(b - \frac{2}{3},\ b,\ b + \frac{2}{3}\right)$. The lower graph represents the real case, with a transverse exponent that is strictly smaller (more attracting). In both cases the function is even, with a sharp minimum at $b = \pm\frac{1}{9}$. The box encloses the region $-1 \le b \le 1$ with $-2.1 \le \mathrm{Lyap}_{\mathcal{F}} \le 1$.

Remark 4.7. (Symmetries.) We conclude this section with some technical remarks. If we permute the three parameters (a, b, c) cyclically, then clearly we obtain a new map $f_{b,c,a}$ that is holomorphically conjugate to $f_{a,b,c}$. We can generalize this construction very slightly by allowing odd permutations also, but changing signs. If S_3 is the symmetric group consisting of all permutations $i \mapsto \sigma_i$ of the three symbols $\{1, 2, 3\}$, then S_3 acts as a group of rotations of $\mathbb{R}^3$ or $\mathbb{C}^3$ as follows: For each $\sigma \in S_3$, consider the *sign-corrected permutation of coordinates* $\widehat{\sigma}(z_1,\, z_2,\, z_3) = \mathrm{sgn}(\sigma)\left(z_{\sigma_1}, z_{\sigma_2},\, z_{\sigma_3}\right)$. Then a brief computation shows that the homogeneous map $F_{a,b,c}$ of $\mathbb{R}^3$ or $\mathbb{C}^3$ is linearly conjugate to the map

$$F_{\widehat{\sigma}(a,b,c)} = \widehat{\sigma} \circ F_{a,b,c} \circ \widehat{\sigma}^{-1}.$$

It follows that the associated map $f_{a,b,c}$ of the projective plane is holomorphically conjugate to the map $f_{\widehat{\sigma}(a,b,c)}$. One can check that these are the only holomorphic conjugacies between Desboves maps (for example, by making use of the eigenvalues of the first derivative of f at the 21 fixed points).

In the complex case, note also that each Desboves map f commutes with a finite group $G \cong \mathbb{Z}/3 \times \mathbb{Z}/3$ of symmetries of the projective plane. In fact, $f \circ g = g \circ f$ for each g in the group G consisting of all automorphisms

$$g(x : y : z) = (\alpha x : \beta y : z) \quad \text{with} \quad \alpha^3 = \beta^3 = 1.$$

Remark 4.8. (A closely related map.) It is sometimes convenient to eliminate these last symmetries by passing to the quotient space $\mathbb{P}^2/G$, which is isomorphic to $\mathbb{P}^2$ itself but with coordinates $(x^3 : y^3 : z^3)$. If we introduce variables $\xi = x^3$, $\eta = y^3$, $\zeta = z^3$, and set $\varphi = \xi + \eta + \zeta$, then the map $(x : y : z) \mapsto (\xi : \eta : \zeta)$ transforms the Fermat curve $\mathcal{F}$ to a line $\varphi = 0$. Under this transformation, the Desboves map (4–1) is semiconjugate to a different rational map

$$(\xi : \eta : \zeta) \\ \mapsto \Big(\xi(\eta - \zeta + a\varphi)^3 : \eta(\zeta - \xi + b\varphi)^3 : \zeta(\xi - \eta + c\varphi)^3)\Big),$$

also of degree four. Evidently this new map carries the line $\varphi = 0$ into itself by a *Lattès map*, that is, the image of a rigid torus map under a holomorphic semiconjugacy. (Compare [Milnor 06a].)

5. EMPIRICAL EXAMPLES

This section will provide empirical discussions of six examples from the Desboves family of degree-four maps, as described in Section 4, plus two examples of lower-degree maps. (Our first example has points of indeterminacy; however, nearby holomorphic maps exhibit very similar behavior.) Four of the six examples from the Desboves family belong to the "two-thirds" subfamily of Definition 4.6.

Note 5.1. (Pictorial conventions.) Each of the color pictures that follow shows the real projective plane represented as a unit 2-sphere with antipodal points identified, oriented as in Figure 1. Thus the x-axis, pointing to the right, and the y-axis, pointing almost vertically, are close to the plane of the paper, while the z-axis points up out of the paper. (Because of this choice of orientation, we will sometimes refer to the coordinate point $(0 : 1 : 0)$ near the top of the picture as the *north pole*.) The Fermat curve $x^3 + y^3 + z^3 = 0$ is traced out in white.

In Figures 3 and 4, other points are colored from red to blue according as their orbits converge more rapidly or more slowly toward this Fermat curve, and subsequent figures use various modifications of this scheme. As an example, in Figure 3 the *equator* $y = 0$ shows up as a blue circle, since orbits in the invariant line $y = 0$ cannot converge to $\mathcal{F}$; hence orbits near this line cannot converge rapidly to $\mathcal{F}$.

In the complex case, we cannot illustrate the map directly. However, the graphs to the right of Figures 3, 4, 5, 6, 10, and 11 describe one more-or-less-typical randomly chosen orbit for the associated complex map. Here each orbit point $(x : y : z)$ has been normalized so that $|x|^2 + |y|^2 + |z|^2 = 1$. The horizontal coordinate measures the number of iterations, while the vertical coordinates in each of the four stacked graphs represent respectively $|x|^2$, $|y|^2$, $|z|^2$, and $|\Phi(x, y, z)|$.

Example 5.2. (The Fermat curve as a global attractor?) If we choose Desboves parameters $\left(b - \frac{2}{3}, b, b + \frac{2}{3}\right)$ with $|b|$ small, then the transverse Lyapunov exponent is negative in both the real and complex cases. Numerical computation suggests that nearly all orbits actually converge to the Fermat curve (perhaps even all but a set of measure zero?).

As an example, consider the case $(a, b, c) = \left(-\frac{2}{3}, 0, \frac{2}{3}\right)$. Using the Gnu multiple-precision arithmetic package, and starting with several thousand randomly chosen points in the real or complex projective plane, we found that all orbits land on the curve, to the specified accuracy, within a few hundred iterations. Of course, even if we could work with infinite-precision arithmetic, such a computation could not prove that a given orbit converges to the curve, and also could not rule out the possibility of other attractors with extremely small basins.

In fact, it seems possible that periodic attractors with high period and small basin exist for a dense open set of parameter values. This case $b = 0$ is rather special in one way, since the map $f_{-2/3,0,2/3}$ has points of indeterminacy, namely those points where $(x^3 : y^3 : z^3)$ is equal to either $(1 : 7 : 1)$ or $(0 : 1 : 0)$.

However, the behavior for small nonzero values of b seems qualitatively similar. In fact, according to Figure 2, which graphs the real and complex transverse Lyapunov exponents, the most attracting case within the two-thirds family occurs for $b = \pm\frac{1}{9}$, which we discuss next.

Example 5.3. (An even stronger attractor.) The case $b = \pm\frac{1}{9}$ yields an even more strongly attracting Fermat curve, as illustrated in Figure 3. The transverse derivative has a simple zero at the point $(-1, 1, 0)/\sqrt{2}$, to the upper left of the figure, and a double zero at the point $(0, -1, 1)/\sqrt{2}$, near the bottom. A numerical search

suggests that this is the most attracting example within the real or complex Desboves family, in the sense that the transverse exponent takes its most negative value of $-2.0404\ldots$ for the real map and $-0.6801\ldots$ for the complex map. Certainly these are the extreme values for real parameters within the two-thirds family, as graphed in Figure 2.

Example 5.4. (Another global attractor?) If we take Desboves coordinates $\left(\frac{1}{3}, 0, -\frac{1}{3}\right)$, then again the Fermat curve seems to attract nearly all orbits. Compare Figure 4. Here the transverse derivative has a double zero at the fixed point $(-1:0:1)$ in the middle of the large red region. It is a curious fact that the transverse exponents in this case are precisely the same as those for Example 5.2, namely $-1.456\ldots$ for the real map and $-0.549\ldots$ for the complex map.

Example 5.5. (A cycle of Herman rings?) Now suppose that we choose Desboves parameters in the two-thirds family, with (a, b, c) equal to $(-\frac{1}{5}, \frac{7}{15}, \frac{17}{15})$. Here the transverse exponent is $-0.509\ldots$ for the real map, but $+0.402\ldots$ for the complex map. Thus we can expect the Fermat curve to be an attractor in the real case, but not in the complex case. The left half of Figure 5 illustrates the dynamics in the real case. Numerical computation suggests that some 83% of the orbits converge to the Fermat curve, while the remaining 17% converge to a pair of small circles. The attractive basin for this pair of circles is conjecturally a dense open subset of $\mathbb{P}^2(\mathbb{R})$. The map $f = f_{a,b,c}$ carries each of these circles to the other, reversing orientation, while $f \circ f$ carries each circle to itself with rotation number $\pm 0.18587\ldots$.

Of course, such a phenomenon can be expected to be highly sensitive to small changes in the parameters—we cannot really distinguish between a rotation circle with irrational rotation number and one with a rational rotation number that has very large denominator (although the latter would necessarily contain a periodic orbit).

In the complex case, the Fermat curve is no longer an attractor. In fact, almost all orbits seem eventually to land near this cycle of circles and then to behave just like an orbit on a pair of nearby circles with the same rotation number. This suggests that most orbits converge to a cycle of two Herman rings in $\mathbb{P}^2(\mathbb{C})$, with the pair of real circles as their central circles. A completely equivalent conjecture would be that these circles are real analytic, or that they are contained in the Fatou set. (For a more detailed discussion of Herman rings in $\mathbb{P}^2(\mathbb{C})$, see Section 8.)

Again we must be cautious, since such a phenomenon must be highly sensitive to perturbations; but the empirical evidence certainly suggests the existence of a cycle of two Fatou components that could only be the immediate basins for attracting Herman rings.[5] (The convergence is very slow, and there may be other much more chaotic attractors.)

These attracting circles persist under small perturbations of the parameters. (Compare Theorem 8.12.) A plot of the rotation number for these circles as a function of the parameter c, keeping a and b fixed, is shown in Figure 7. If these circles remain real analytic, under suitable conditions on the rotation number, then we would have a cycle of two Herman rings for many nearby maps. It seems empirically that this is true, but we have been unable to prove it. (Compare Remark 8.14.)

Example 5.6. (The line $z = 0$ as a measure-theoretic attractor?) See Figure 6. For the parameter values $(a, b, c) = (-1.4, -0.8, 1.4)$, the Lyapunov exponent turns out to be strictly positive, equal to $0.247\ldots$ in the real case and to $0.352\ldots$ in the complex case. The invariant Fermat curve does not seem to play any significant dynamical role in this case. On the other hand, the equator $y = 0$ seems to be at least a measure-theoretic attractor, and there is also an attracting fixed point at the north pole $(0:1:0)$. In fact, many randomly chosen real or complex orbits converge to the north pole $(0:1:0)$, but even more seem to converge to the equator.

Example 5.7. (A composite statistical attractor?) For the real or complex map with Desboves parameters $\left(\frac{1}{3}, 1, \frac{5}{3}\right)$, as illustrated in Figure 10 for the real case, typical orbits seem to spend a great deal of time quite close to the Fermat curve $\mathcal{F}$ even though the transverse exponent is strictly positive, equal to $0.081\ldots$ in the real case and to $1.032\ldots$ in the complex case. This curve by itself is only a "transient attractor," since nearby orbits often seem to be attracted but eventually get kicked away from it. However, the union

$$A = \{x = 0\} \cup \{y = 0\} \cup \{z = 0\} \cup \mathcal{F}\,,$$

or in other words, the variety $xyz\,\Phi(x, y, z) = 0$, does seem to behave like an attractor, at least in a statistical

[5] These conjectured Herman rings cannot extend to Siegel disks. For if there were such an extension, then this disk together with its complex conjugate would yield an immersed curve $\mathcal{C}$ of genus zero, mapped to itself by an irrational rotation, so that $\deg f|_{\mathcal{C}} = 1$. Such a curve would be algebraic by Chow's theorem [Chow 49]; but this situation is impossible by the discussion in Definition 2.1.

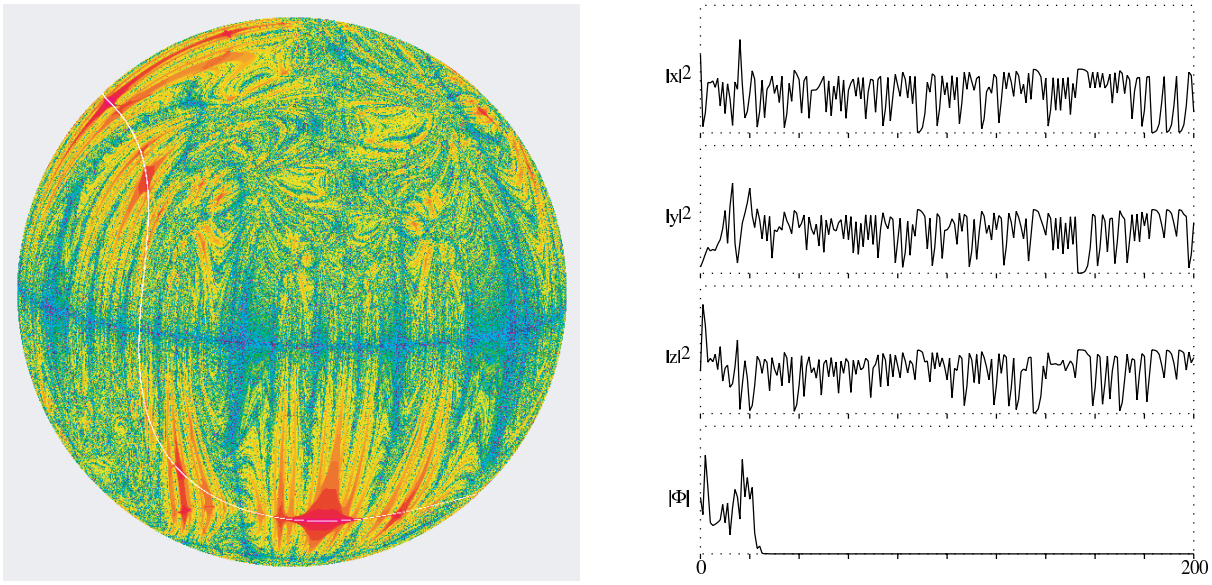

FIGURE 3. (See Example 5.3.) On the left: dynamics on the real projective plane for the Desboves map in the two-thirds family with parameters $(a, b, c) = (-\frac{5}{9}, \frac{1}{9}, \frac{7}{9})$. The sphere is oriented as in Figure 1. On the right: plot of $|x|^2$, $|y|^2$, $|z|^2$, and $|\Phi|$ as functions of the number of iterations for a typical randomly chosen complex orbit. Here each orbit point $(x : y : z)$ has been normalized so that $|x|^2 + |y|^2 + |z|^2 = 1$. In this run, it took 23 iterations to come close enough to the Fermat curve so that $|\Phi|$ appears to be zero on the graph.

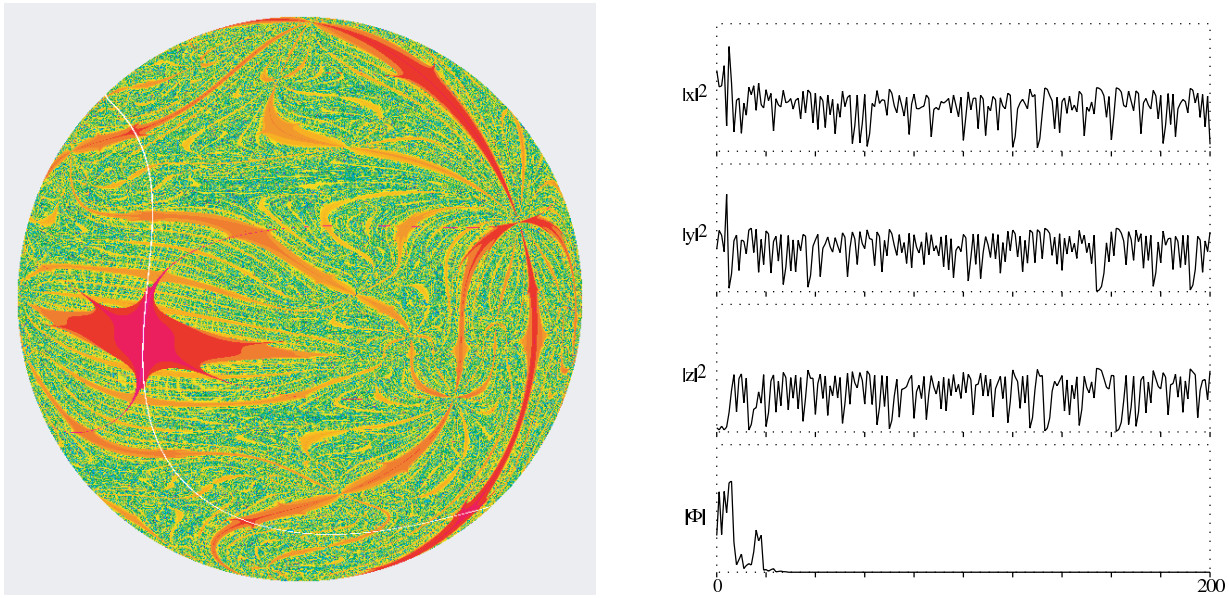

FIGURE 4. (See Example 5.4.) For the map with Desboves parameters $(\frac{1}{3}, 0, -\frac{1}{3})$, the Fermat curve again seems to attract all or nearly all orbits in both the real and complex cases.

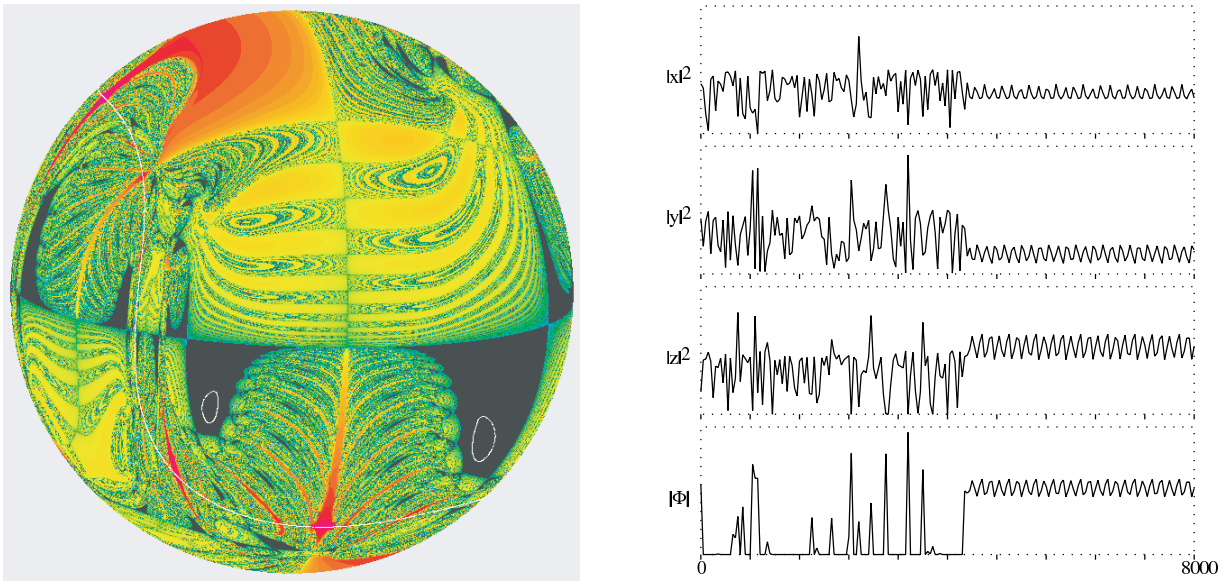

FIGURE 5. (See Example 5.5.) Dynamics for the parameters $(-\frac{1}{5}, \frac{7}{15}, \frac{17}{15})$. Left: In the real case there are two attractors. The basin of the Fermat curve is colored as in Figures 3, 4. However, the two small white circles also form an attractor. The corresponding basin is shown in dark gray. Right: A typical randomly chosen orbit for the complex map. This orbit often comes very close to the Fermat curve during the first four thousand iterations but then seems to converge to a cycle of two Herman rings.

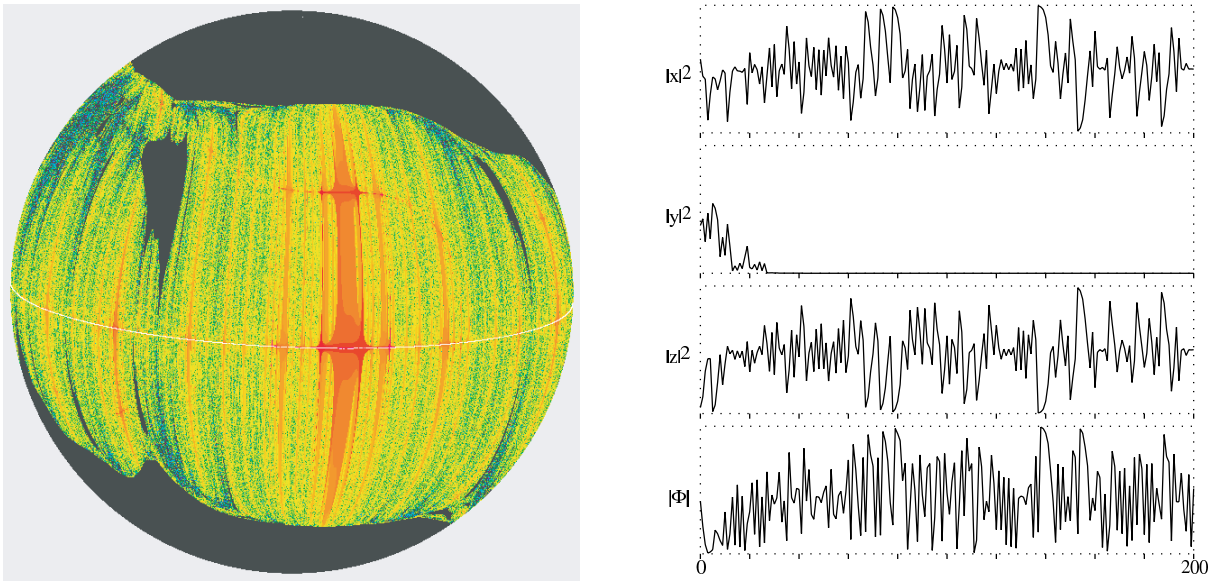

FIGURE 6. (See Example 5.6.) Plots for the map with Desboves parameters $(-1.4\,,\ -.8\,,\ 1.4)$. Here the coloring is as in the previous figures except that it describes convergence to the "equator" $y = 0$, rather than to the invariant Fermat curve. For this map, the "north pole" $(0 : 1 : 0)$ also attracts many orbits.

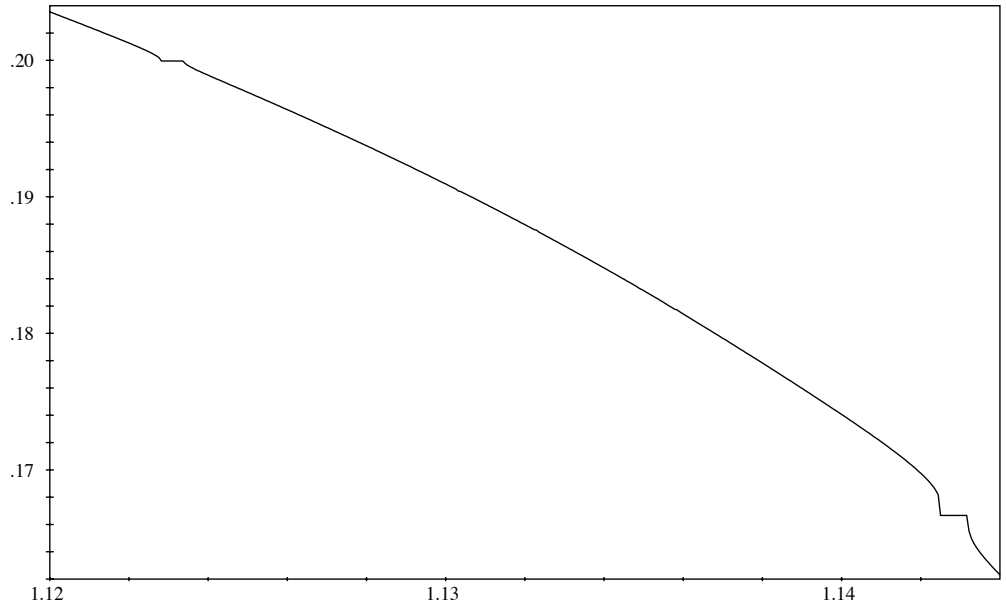

FIGURE 7. An empirical plot of the rotation number for the pair of attracting circles in $\mathbb{P}^2(\mathbb{R})$ as a function of the parameter c in Example 5.5, keeping a and b fixed. Presumably, for each rational value for the rotation number there corresponds an entire plateau of c values for which the pair of circles contains an attracting periodic orbit. Only the plateaus of height $\frac{1}{5}$ and $\frac{1}{6}$ are visible in this figure; but with higher resolution, tiny blips at height $\frac{3}{16}$ and $\frac{2}{11}$ would also be visible. As c decreases past 1.12, the attracting circles shrink to points, while as c increases past 1.144, they expand until they break up upon hitting the boundary of their attracting basin. It is conjectured that whenever the rotation number is Diophantine, the corresponding pair of circles in $\mathbb{P}^2(\mathbb{R})$ are contained in a pair of Herman rings in $\mathbb{P}^2(\mathbb{C})$.

sense. (Compare Remark 5.8.) Typical orbits seem to spend most of the time extremely close to this variety.

However, they do not stay in any one of its four irreducible components, but sometimes jump from one component to another. Furthermore, it seems likely that typical orbits will escape completely from a neighborhood of this variety, very infrequently but infinitely often.

Here is a more detailed description, as illustrated in Figure 8. To fix ideas, we will refer to the real case; but the complex case is not essentially different. A randomly chosen orbit seems to spend most of the time either wandering chaotically very close to the Fermat curve or else remaining almost stationary, very close to one of the four saddle fixed points (the black dots in Figure 8).

However, such an orbit does not seem to stay close to any one of the four components of this variety forever. For example, it is likely to escape from the neighborhood of the Fermat curve $\mathcal{F}$ when it comes very close to the strongly repelling point $\mathcal{F} \cap \{y = 0\}$, which is circled in Figure 8. It will then shadow the coordinate line $y = 0$, jumping quickly to a small neighborhood of the saddle point $x = y = 0$ and then slowly coming closer to this point for thousands of iterates. Again it must eventually escape, now shadowing the line $x = 0$ and jumping quickly either toward the saddle point $\mathcal{F} \cap \{x = 0\}$ or toward the saddle point $x = z = 0$.

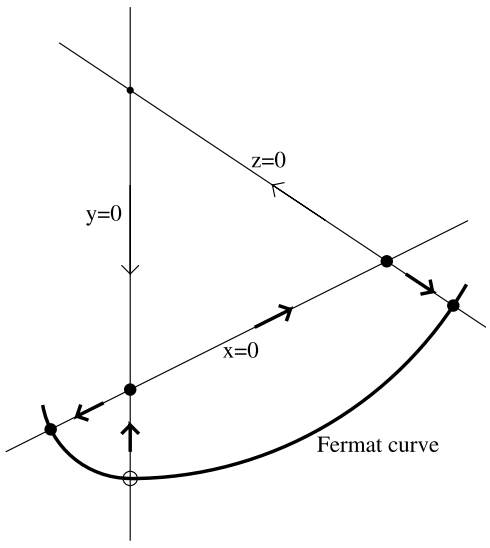

FIGURE 8. Schematic diagram illustrating Example 5.7.

In either case it again spends a long time approaching this saddle point, but then escapes. In the first case, it is now very close to the Fermat curve and shadows it for a long time with a highly chaotic orbit before starting the cycle again. In the second case, in which it escapes near the saddle point $x = z = 0$, it then shadows the line $z = 0$ as it quickly converges toward the saddle point $\mathcal{F} \cap \{z = 0\}$, where it again remains for a long time before repeating the cycle.

Remark 5.8. (Statistical attractors.) Such examples have led authors such as those of [Gorodetski and Ilashenko 96] and [Ashwin et al. 98] to suggest modified definitions of attractor, emphasizing not the omega-limit set of a typical orbit, but rather its asymptotic probability distribution. As a typical example, think of a dynamical system in the plane in which orbits spiral out toward a limit cycle Γ that consists of a homoclinic loop, beginning and ending at a fixed point p. Then the unique "measure-theoretic attracting set" for the region inside the loop is the entire loop Γ. No orbit starting inside actually converges to the point p. However, every orbit starting inside the loop spends most of its time apparently converging to p, with a statistically insignificant (but infinite) collection of exceptional times. Thus Gorodetski and Ilyashenko, or Ashwin, Aston, and Nicol, describe this point p as a "statistical attractor." Here is a more formal definition, which makes sense in any smooth compact manifold (provided with a metric for convenience). By definition, an orbit $\{x_n\}$ *converges* toward a compact set A if the distance $d(x_n, A)$ tend to zero as $n \to \infty$.

Definition 5.9. The orbit $x_0 \mapsto x_1 \mapsto \cdots$ *converges statistically* toward A if the time average of distances tends to zero:[6]

$$\frac{1}{n}\big(d(x_0, A) + d(x_1, A) + \cdots + d(x_{n-1}, A)\big) \to 0$$

as $n \to \infty$.

Thus occasional orbit points are allowed to wander away from A, as long as most of them converge. Now given a preferred measure on the ambient space, we can describe A as a (minimal) *statistical attractor* if the union of orbits that converge statistically to A has positive measure, and if no smaller compact set has this property. In particular, in Example 5.7, we conjecture that the Fermat curve, together with the two isolated points where $x = 0$ and $yz = 0$, forms a statistical attractor (and perhaps even a "global" one, statistically attracting everything outside of a set of measure zero).

[6]Since the ambient space is compact, an equivalent condition is that every point $q \notin A$ has a neighborhood U such that $(1/n)\big(\chi_U(x_0) + \chi_U(x_1) + \cdots + \chi_U(x_{n-1})\big) \to 0$ as $n \to \infty$, where $\chi_U : \mathbb{P}^2 \to \{0, 1\}$ is the characteristic function of U.

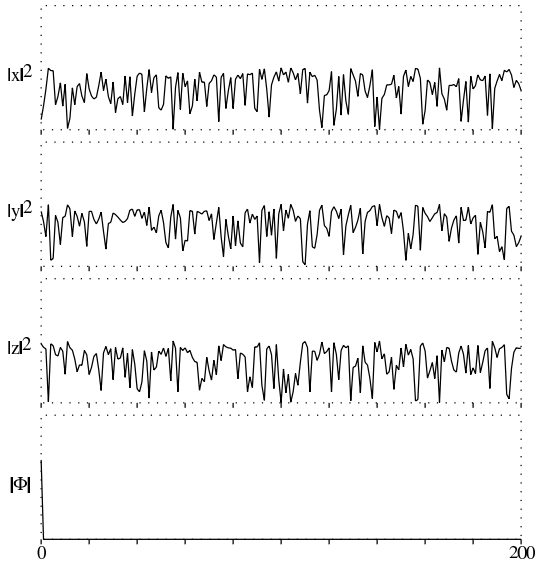

FIGURE 9. A plot of 200 iterations with a random start for the degree-three map of Example 5.10, taking parameters $(a, b, c) = (0, \gamma, -1)/2$.

Example 5.10. (A family of degree-three maps.) In the case of a map of degree three (or indeed for any degree that is not a perfect square), the multiplier on an invariant elliptic curve cannot be a real number. Hence we can consider only the complex case; we cannot describe both the map and the invariant curve by equations with real coefficients.

Here is one explicit family of complex degree-three maps that send the Fermat curve $\mathcal{F}$ into itself [Bonifant and Dabija 02, p. 17]. As in Section 4, we start with a rather degenerate self-map of $\mathbb{P}^2$. Let

$$H_0(x, y, z) = \left(\ell xyz, y^3 - \gamma z^3, z^3 - \gamma y^3\right),$$

where γ is the cube root of unity $(-1+i\sqrt{3})/2$ and where $\ell^3 = 3(\gamma^2 - \gamma)$. (For example, $\ell = 1 - \gamma$ or $\ell = i\sqrt{3}$.) Then the associated map

$$h_0(x : y : z) = \left(\ell xyz : y^3 - \gamma z^3 : z^3 - \gamma y^3\right)$$

of projective space has a first integral Φ/Ψ, where $\Phi(x, y, z) = x^3 + y^3 + z^3$ and $\Psi(x, y, z) = x^3$. In fact, a brief computation shows that

$$\begin{aligned}\Phi(H_0(x, y, z))/\Phi(x, y, z) &= \Psi(H_0(x, y, z))/\Psi(x, y, z) \\ &= 3y^3z^3\,,\end{aligned}$$

and it follows immediately that the rational function Φ/Ψ is invariant under h_0. In particular, the Fermat curve defined by $\Phi = 0$ is h_0-invariant. However, in contrast to the Desboves case of Section 4, the various elliptic curves $\Phi/\Psi = \text{constant} \in \mathbb{C}\smallsetminus\{1\}$ are all mutually isomorphic. (A similar example will be described in Remark 6.9.) The map h_0 has just one point of indeterminacy, namely $(1 : 0 : 0)$, and this point is not on $\mathcal{F}$.

Like all maps of $\mathbb{P}^2$ with first integral, h_0 is not very interesting as a dynamical system (see Lemma 3.1), but it does embed in a family of more-interesting maps. Consider the 3-parameter family of homogeneous polynomials

$$H = H_{a,b,c} = H_0 + (a, b, c)\Phi.$$

Each of the associated maps $h_{a,b,c}$ of the projective plane carries the Fermat curve $\mathcal{F}$ to itself with degree three and multiplier $\gamma\ell$. There is only one fixed point of $h_{a,b,c}$ on $\mathcal{F}$, namely $(0 : -1 : 1)$.

First consider the one-complex-parameter subfamily of degree-three maps satisfying the conditions

$$a = b + \gamma c = 0,$$

with $x = 0$ as invariant line. (The use of these special parameters simplifies the computation of the transverse Lyapunov exponent.) When $b = \gamma/2$, the transverse Lyapunov exponent takes its most negative value of -1.647918. Thus $\mathcal{F}$ appears to be more strongly attracting under this map than under any of the complex Desboves maps, where the most negative transverse exponent was $-0.6801\ldots$. (See Example 5.3; such computations will be explained in Part 2 of this paper.) In Figure 9, we illustrate the extraordinary attracting properties of the Fermat curve for this map. Most randomly chosen points seemed to hit the Fermat curve, up to the resolution of the graph, after only six or so iterations. (Compare with the right-hand sides of Figures 3, 4, and 11.)

It is also interesting to consider the subfamily consisting of maps $h_{a,0,0}$ with $b = c = 0$. These are "elementary maps" (Definition 6.1). For this particular elementary family, we suspect on the basis of computer experiments that the transverse exponent is always nonnegative, so that the Fermat curve is never an attractor.

Example 5.11. (The degree-two case.) According to [Bonifant and Dabija 02, Proposition 6.6], up to holomorphic conjugacy, there are exactly 20 distinct examples of holomorphic self-maps of $\mathbb{P}^2(\mathbb{C})$ of algebraic degree two with an invariant elliptic curve (or 10 distinct examples up to complex conjugacy). See Example 6.9 of their paper for a detailed study of one of these degree-two maps. (We have not tried to study the other cases.) In this example, with multiplier equal to $i\sqrt{2}$, there are five attracting cycles, with common basin boundary equal to the Julia set. Four of these are attracting fixed points, and the fifth is an attracting period-2 orbit. Empirically, randomly chosen orbits for this example always seem to converge to one of these five cycles.

6. INTERMINGLED BASINS

Finally, we come to examples in which we can provide complete proofs.

Definition 6.1. A rational self-map f of $\mathbb{P}^2$ with $\deg(f) > 1$ is called *elementary* with *center* ϱ_0 if it leaves invariant the pencil of lines passing through ϱ_0, i.e., every line through ϱ_0 maps to a line through ϱ_0.

Elementary maps are easier to analyze than more-general rational maps, since we can separate the variables to simplify the discussion.

Example 6.2. (Elementary Desboves maps.) In particular, consider a Desboves map $f = f_{a,b,c}$ as in formula (4–1) of Section 4, where the parameters a, b, c satisfy $a = -1$ and $c = 1$. Then the image $f(x : y : z) = (x' : y' : z')$ satisfies

$$x' = x(-x^3 - 2z^3) \quad \text{and} \quad z' = z(2x^3 + z^3).$$

It follows that each line $(x : z) = \text{constant}$ through the coordinate point $\varrho_0 = (0 : 1 : 0)$ maps to another line $(x' : z') = \text{constant}'$ through ϱ_0. If we set $X = x/z$ and $X' = x'/z'$, then the correspondence

$$\widehat{f} : X \mapsto X' = -X\frac{X^3 + 2}{2X^3 + 1} \tag{6–1}$$

does not depend on the choice of b. This rational map (6–1) is described as a *Lattès map*, since it is the image of a rigid map on the torus $\mathcal{F} \cong \mathbb{C}/\Omega$ under the semiconjugacy $(x : y : z) \mapsto (x : z)$ of degree three. (In fact, $\widehat{f}$ is conformally conjugate to the Lattès map described in Remark 4.8.) It has an ergodic invariant measure that is smooth except at its critical values, the cube roots of -1. Over the real numbers, $\widehat{f}$ is a covering map from the circle $\mathbb{P}^1(\mathbb{R})$ to itself with topological degree -2.

Over either the real or complex numbers, if we think of $\mathbb{P}^2\smallsetminus\{\varrho_0\}$ as a (real or complex) line bundle over the

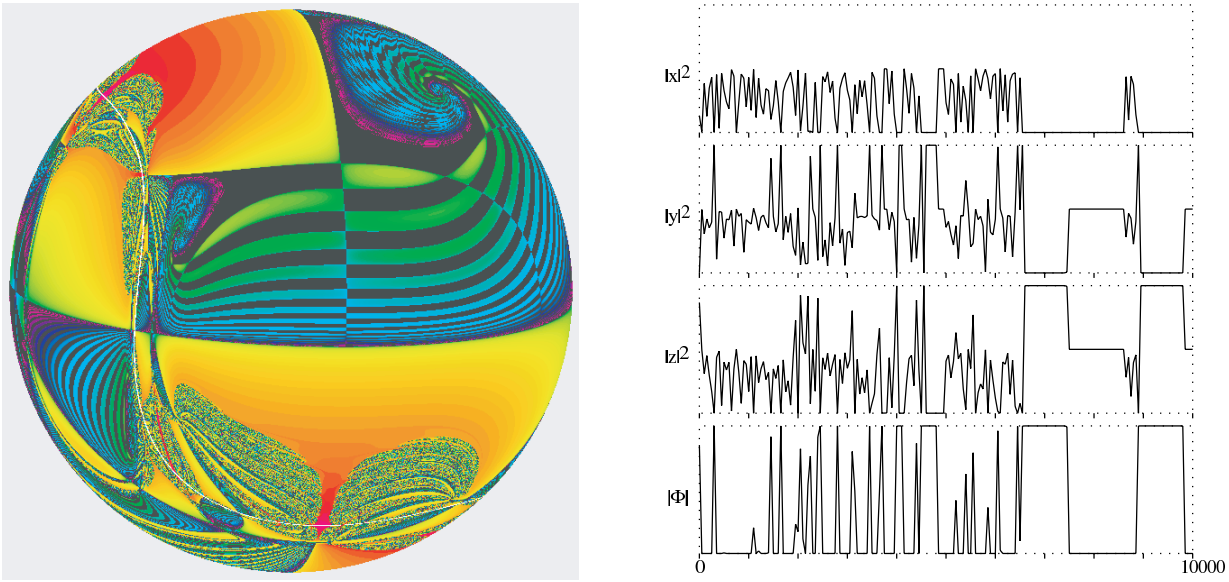

FIGURE 10. (See Example 5.7.) On the left: Corresponding figure for the real Desboves map with parameters $(\frac{1}{3}, 1, \frac{5}{3})$, again describing convergence to (or at least coming close to) the Fermat curve. On the right: One randomly chosen orbit for the complex map through 10000 iterations.

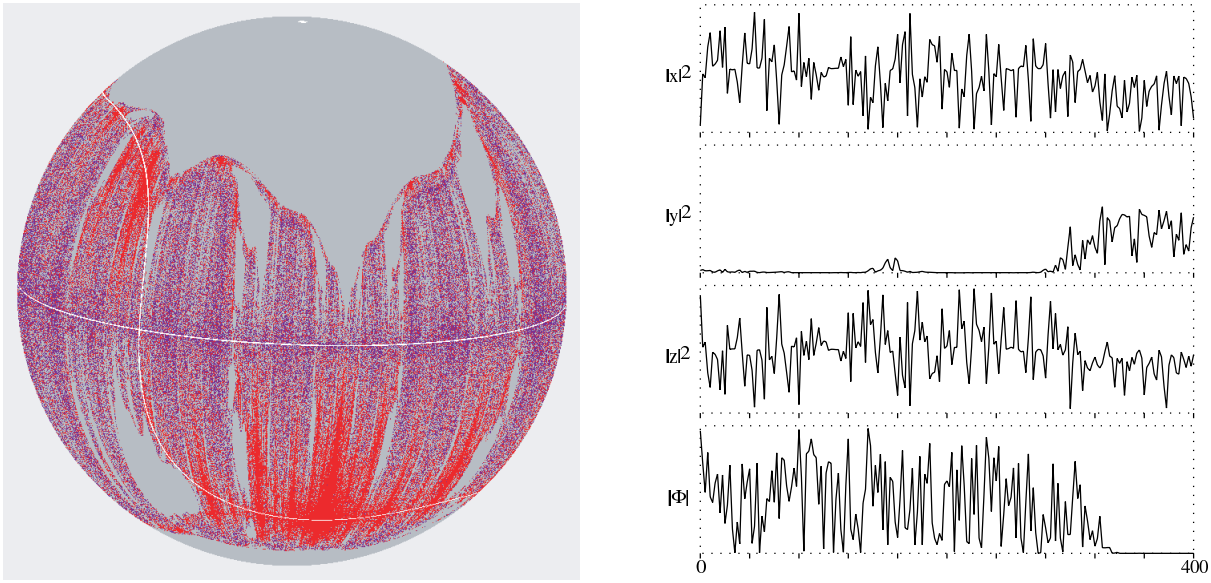

FIGURE 11. (See Remark 6.6.) Plots for the "elementary map" with parameters $(a, b, c) = \left(-1, \frac{1}{3}, 1\right)$. In this case, every great circle through the north pole $(0 : 1 : 0)$ maps to a great circle through the north pole. There are three attractors: the Fermat curve $\mathcal{F}$, the equator $\{y = 0\}$, and the north pole, each marked in white. The corresponding attracting basins are colored red, blue, and gray respectively. (However, the closely intermingled blue and red yield a purple effect.) The graphs on the right show an orbit that nearly converges to $\{y = 0\}$ but then escapes toward $\mathcal{F}$.

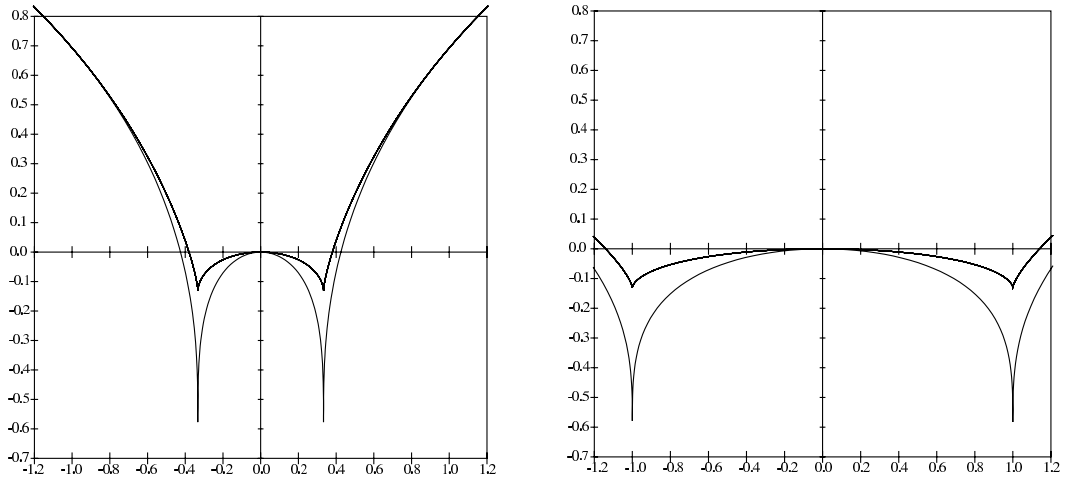

FIGURE 12. On the left: plot of the transverse Lyapunov exponent along the Fermat curve as a function of the parameter b for the elementary family of Example 6.2, with Desboves parameters $(-1, b, 1)$. On the right: corresponding plot for the transverse exponent along the line $y = 0$. In both cases, the graph for the complex map lies above the graph for the real map.

projective line $\mathbb{P}^1$ with projection $\Pi : (x : y : z) \mapsto (x : z)$, then we have the commutative diagram

$$\begin{array}{ccc} \mathbb{P}^2 \smallsetminus \{\varrho_0\} & \stackrel{f}{\to} & \mathbb{P}^2 \smallsetminus \{\varrho_0\} \\ \Pi \downarrow & & \Pi \downarrow \\ \mathbb{P}^1 & \stackrel{\widehat{f}}{\to} & \mathbb{P}^1 \end{array}$$

where f carries each fiber into a fiber by a polynomial map, with coefficients that vary with the fiber. As an example, for the two invariant fibers $x = 0$ and $z = 0$, we get the maps

$$(0 : y : 1) \mapsto (0 : by^4 + (1 + b)y : 1),$$
$$(-1 : y : 0) \mapsto (-1 : by^4 + (1 - b)y : 0),$$

respectively. If we exclude the degenerate case $b = 0$ (compare Remark 6.9), then these polynomial maps all have degree four. Furthermore, the center point $\varrho_0 = (0 : 1 : 0)$ is superattracting, and serves as the point at infinity for each one. In the real case, these polynomial maps are all unimodal, while in the complex case they all have 120° rotational symmetry.

Since the rational map $\widehat{f}$ of the base space has no attracting cycles, it follows that an elementary map with invariant elliptic curve can have no attracting cycles other than its center point.

In the special case of an elementary map, we can give a relatively easy proof that a negative transverse exponent for any invariant elliptic curve implies that this curve is a measure-theoretic attractor. Furthermore, in the case of an elementary Desboves map f we get a surprising bonus: *The invariant line $\{y = 0\}$ is also carried into itself, and the resulting self-map is conjugate to the Lattès map of* (6–1). *Hence it also has a canonical ergodic invariant measure and a well-defined transverse Lyapunov exponent.*

According to Figure 12, for real values of b, both of these transverse exponents are strictly negative, provided that $|b|$ is fairly small and nonzero; hence the following theorem will imply that both the Fermat curve and the line $\{y = 0\}$ are measure attractors. For example, this is the case for the elementary Desboves map with parameter $b = \frac{1}{3}$, corresponding to a minimum point in the left-hand diagram of Figure 12. (Compare Figure 11.)

Theorem 6.3. (Basins of positive measure.) *Let f be a real or complex elementary map with an invariant elliptic curve $\mathcal{C}$. If the transverse Lyapunov exponent* $\mathrm{Lyap}_{\mathcal{C}}$ *is strictly negative, then the attracting basin $B(\mathcal{C})$, consisting of points whose orbit converges to $\mathcal{C}$, has strictly positive measure. In fact, any neighborhood of a point of $\mathcal{C}$ intersects $B(\mathcal{C})$ in a set of positive measure.*

Similarly, if such an f has an invariant line $\mathcal{L}$ not passing through the center, with strictly negative transverse exponent, then the attracting basin for this line has positive measure and intersects any neighborhood of a point of this line in a set of positive measure.

In the complex case we can give a much more precise picture. (As usual, define the Fatou and Julia sets as in Definition 1.3.) If p is any point of an invariant elliptic curve, then according to [Bonifant and Dabija 02, Theo-

rem 5.4 and Proposition 6.16], the iterated preimages of p are everywhere dense in the Julia set (see Remark 4.3), and furthermore, we have the following proposition.

Proposition 6.4. (The Fatou set is a dense open basin.) *If f is a complex elementary map with an invariant elliptic curve, and if the center ϱ_0 is not a point of indeterminacy, then ϱ_0 is a superattracting fixed point whose basin coincides with the Fatou set. This basin is connected and everywhere dense in $\mathbb{P}^2$. Furthermore, if U is a small neighborhood of a point of the Julia set, then the union of the forward images of U is the entire space $\mathbb{P}^2 \smallsetminus \{\varrho_0\}$.*

Proof: A proof can be found in [Bonifant and Dabija 02, p. 18]. □

In particular, the conjectured Lemma 4.5 is true in this case: the attracting basin for the elliptic curve has no interior points. Similarly, if there is an invariant line $\mathcal{L}$ disjoint from the center ϱ_0, then the attracting basin of $\mathcal{L}$ cannot have any interior point. It also follows that f is topologically transitive on the Julia set. This means that the orbit of a "generic" point of the Julia set J is everywhere dense in J. Such a generic point of J cannot belong to any of the attracting basins $B(\mathcal{C})$, $B(\mathcal{L})$, $B(\varrho_0)$.

Corollary 6.5. (Intermingled basins.) *If a complex elementary map has both an invariant line $\mathcal{L}$ that does not pass through its center and an invariant elliptic curve $\mathcal{C}$, then the two topological closures $\overline{B(\mathcal{C})}$ and $\overline{B(\mathcal{L})}$ are both precisely equal to the Julia set. Furthermore, if the transverse Lyapunov exponent for $\mathcal{C}$ (or for $\mathcal{L}$) is negative, then every neighborhood U of a point of the Julia set intersects $B(\mathcal{C})$ (or respectively $B(\mathcal{L})$) in a set of positive Lebesgue measure.*

Remark 6.6. (Three basins.) In the case that the transverse exponents $\mathrm{Lyap}_{\mathcal{C}}(f)$ and $\mathrm{Lyap}_{\mathcal{L}}(f)$ are both negative, it follows that the basins for these two attractors are intimately intermingled. For the real Desboves map illustrated in Figure 11, a very rough estimate suggests that about 66% of the points in $\mathbb{P}^2$ are attracted to the center $(0:1:0)$, about 17% to the line $\{y=0\}$, and about 17% to the Fermat curve. For the associated complex mapping, the figures are 81%, 13%, and 6%. (However, the computation is highly sensitive, and these estimates may well be quite inaccurate.) It may be conjectured that every point outside of a set of measure zero lies in the union of these three attracting basins.

Remark 6.7. (Terminology.) Such exotic behavior has been studied extensively, particularly in the applied dynamics literature. The term "riddled basin" was introduced in [Alexander et al. 92] to indicate an attracting basin whose complement intersects every disk in a set of positive measure. The authors define two basins to be *intermingled* if every disk that intersects one basin in a set of positive measure also intersects the other basin in a set of positive measure. For a particularly clear example, see [Kan 94]. Such examples of intermingled basins seem to be known only in cases in which the attractors themselves are quite smooth. We don't know whether there can be two fractal attractors whose basins have the same closure.

Proof of Theorem 6.3: Without loss of generality, we may assume that the center ϱ_0 of the real or complex elementary map f is $(0:1:0) \notin \mathcal{I}_f$. Furthermore, if there is an invariant line not passing through this center, we may assume that it is the line $\{y=0\}$, as in Figure 11. (Since we assume that there is an invariant elliptic curve $\mathcal{C}$, it follows that any invariant line not passing through the center is mapped to itself by a Lattès map, with an absolutely continuous invariant measure, so that the transverse Lyapunov exponent is well defined.)

Each fiber $(x:z) = \text{constant}$ of the fibration $\Pi(x:y:z) = (x:z)$ can be provided with a flat metric

$$\frac{|dy|}{\sqrt{|dx|^2+|dz|^2}}, \tag{6–2}$$

which gives rise to a norm $\|\vec{v}\,\|_{\mathrm{t}}$ for vectors tangent to the fiber. Let

$$\|f'_{\mathrm{t}}(p)\| = \|f'\vec{v}\,\|_{\mathrm{t}}/\|\vec{v}\,\|_{\mathrm{t}}$$

be the norm of the partial derivative along the fiber, where $\vec{v}$ can be any nonzero vector tangent to the fiber at p. (Note that any vector tangent to its fiber must map to a vector tangent to the image fiber.) This norm is well defined, depending only on the base point p of $\vec{v}$. At points of the curve $\mathcal{C}$, we want to compare $\|\vec{v}\,\|_{\mathrm{t}}$ with the semidefinite norm $\|\vec{v}\,\|_{\pitchfork}$, which is obtained by first projecting $\vec{v}$ to the quotient vector space $T(\mathbb{P}^2,p)/T(\mathcal{C},p)$ and then using a positive definite norm in this quotient space.

Note that most fibers intersect the degree-three curve $\mathcal{C}$ transversally in three distinct points. There is only a finite number of exceptional fibers that intersect tangentially. Therefore, the ratio $\|\vec{v}\,\|_{\pitchfork}/\|\vec{v}\,\|_{\mathrm{t}} \geq 0$ is a continuous function on $\mathcal{C}$ that vanishes only at these points of tangency.

Furthermore, the logarithm $\ell(p)$ of this ratio has only logarithmic singularities, and hence is an integrable function on $\mathcal{C}$. Since the measure $d\lambda$ is f-invariant, it follows that the difference

$$\int_{\mathcal{C}} \log \|f'_{\pitchfork}\| d\lambda - \int_{\mathcal{C}} \log \|f'_{\mathrm{t}}\|\, d\lambda = \int_{\mathcal{C}} \ell \circ f d\lambda - \int_{\mathcal{C}} \ell\, d\lambda$$

is zero. In other words, the average value $\int_{\mathcal{C}} \log \|f'_{\mathrm{t}}\|\, d\lambda$ coincides with the transverse exponent $\mathrm{Lyap}_{\mathcal{C}}$ of Section 2.

For any p and q belonging to the same fiber, let $\delta(q,p) \geq 0$ be the distance of q from p, using the flat metric of (6–2) on this fiber. Then

$$\delta(f(q), f(p)) = \|f'_{\mathrm{t}}(p)\| \delta(q,p) + o(\delta(q,p))$$

as $\delta(q,p)$ tends to 0. This estimate holds uniformly throughout a neighborhood of $\mathcal{C}$. Hence, given any $\epsilon > 0$, we can choose δ_0 such that

$$\delta(f(q), f(p)) \leq \big(\|f'_{\mathrm{t}}(p)\| + \epsilon\big)\, \delta(q,p) \tag{6–3}$$

when $p \in \mathcal{C}$ and $\delta(q,p) < \delta_0$ with $\Pi(p) = \Pi(q)$.

Choose ϵ small enough that

$$\int_{\mathcal{C}} \log \big(\|f'_{\mathrm{t}}(p)\| + \epsilon\big)\, d\lambda(p) < 0. \tag{6–4}$$

Let $p_0 \mapsto p_1 \mapsto \cdots$ be the orbit of an arbitrary initial point $p_0 \in \mathcal{C}$ under f. By the Birkhoff ergodic theorem, the averages

$$\frac{1}{n}\Big(\log(\|f'_{\mathrm{t}}(p_0)\| + \epsilon) + \log(\|f'_{\mathrm{t}}(p_1)\| + \epsilon) + \cdots + \log(\|f'_{\mathrm{t}}(p_{n-1})\| + \epsilon)\Big)$$

converge to the integral of (6–4) for almost all $p_0 \in \mathcal{C}$.

In particular, for almost all p_0 it follows that the number

$$\log \big(\|f'_{\mathrm{t}}(p_0)\| + \epsilon\big) + \log \big(\|f'_{\mathrm{t}}(p_1)\| + \epsilon\big) + \cdots + \log \big(\|f'_{\mathrm{t}}(p_{n-1})\| + \epsilon\big)$$

is negative for large n. Thus the n-fold product

$$\big(\|f'_{\mathrm{t}}(p_0)\| + \epsilon\big) \cdots \big(\|f'_{\mathrm{t}}(p_{n-1})\| + \epsilon\big)$$

is less than one for large n, but equal to one by definition for $n = 0$. It follows that the maximum

$$M(p_0) = \max_{n \geq 0} \Big(\big(\|f'_{\mathrm{t}}(p_0)\| + \epsilon\big)\big(\|f'_{\mathrm{t}}(p_1)\| + \epsilon\big) \times \cdots \times \big(\|f'_{\mathrm{t}}(p_{n-1})\| + \epsilon\big)\Big) \geq 1$$

is well defined, measurable, and finite almost everywhere. If $\delta(q,p_0) \leq \delta_0/M(p_0)$, then it follows from the inequality of (6–3) that $\delta\big(f^{\circ n}(q),\, f^{\circ n}(p_0)\big) \leq \delta_0$ for all n, and also that this distance converges to zero as $n \to \infty$.

Now let S be the set of positive measure consisting of all q with $\delta(q,p) \leq \delta_0/M(p)$ for some $p \in \mathcal{C}$ with $\Pi(p) = \Pi(q)$. (Here $\delta_0/\infty = 0$ by definition.) Then for all $q \in S$ it follows that the orbit of q converges to $\mathcal{C}$. Evidently, S intersects every neighborhood of a point of $\mathcal{C}$ in a set of positive measure. The proof for the basin of the line $y = 0$ is completely analogous. □

Remark 6.8. (What about positive transverse exponent?) Conversely, it seems natural to conjecture that the basin of $\mathcal{C}$ has measure zero whenever the transverse Lyapunov exponent is positive. One might guess that this could be proved simply by reversing the inequalities in the argument above, but this doesn't work. The problem is that $\log\big(\|f'_{\mathrm{t}}\| - \epsilon\big)$ is not a meaningful approximation to $\log \|f'_{\mathrm{t}}\|$, since $\|f'_{\mathrm{t}}\|$ must sometimes be smaller than any given ϵ. In fact, almost every orbit near $\mathcal{C}$ must pass arbitrarily close to the critical locus of f. But whenever p is very close to the critical locus, there is a real possibility that $f(p)$ will be much closer to $\mathcal{C}$ than would have been predicted from the differential inequality.

It seems unlikely that this effect could be strong enough to make $\mathcal{C}$ a measure-theoretic attractor in some cases in which the transverse Lyapunov exponent is positive, but we don't know how to rule out this possibility. (Compare Remark 1.4.)

Proof of Corollary 6.5: It follows immediately from Proposition 6.4 that the basins of $\mathcal{C}$ and $\mathcal{L}$ are contained in the Julia set. On the other hand, if $p \in \mathcal{C} \cap \mathcal{L}$, then the iterated preimages of p are contained in both basins, and are dense in J. (Compare Remark 4.3.) Therefore, the closure of either basin is equal to J.

If the open set U intersects the Julia set, then it contains an iterated preimage of p. Since f is an open mapping, it follows that some forward image $f^{\circ n}(U)$ is an open neighborhood of p. If $\mathcal{C}$ (or $\mathcal{L}$) has negative transverse exponent, then by Theorem 6.3, the image $f^{\circ n}(U)$ intersects the corresponding basin in a set of positive measure. Choosing a regular value of $f^{\circ n}$ that is a point of density for this intersection, and choosing a point $q \in U$ that maps to this regular value, it follows easily that any neighborhood of q intersects the corresponding basin in a set of positive measure. □

Remark 6.9. (The special case $b = 0$.) The above discussion of elementary Desboves maps $f = f_{-1,b,1}$ always assumed that the parameter b is nonzero. For the case $b = 0$, we have a much simpler situation. The center $(0 : 1 : 0)$ then becomes a point of indeterminacy. If we think of each fiber V as a one-dimensional complex vector space, taking $V \cap \mathcal{L}$ to be its zero vector, then each fiber maps linearly to a fiber. In fact, it is not hard to see that f is well defined as a holomorphic map from the complement $\mathbb{P}^2 \setminus \{(0 : 1 : 0)\}$ onto itself, and that this complement is "foliated" by f-invariant curves $x^3 + ky^3 + z^3 = 0$, which are isomorphic to the Fermat curve for $k \in \mathbb{C} \setminus \{0\}$. (In particular, the map $f = f_{-1,0,1}$ has a first integral. Compare Lemma 3.1.) These invariant curves intersect only in the finite set $\mathcal{F} \cap \mathcal{L}$.

7. TRAPPED ATTRACTORS: EXISTENCE AND NONEXISTENCE

The first half of this section will provide explicit examples of everywhere-defined rational maps of $\mathbb{P}^2(\mathbb{R})$ that have a smoothly immersed real curve of genus one as trapped attractor (Definition 1.1). The second half will prove that a complex curve of genus one can never be a trapped attractor.

Example 7.1. (A singular real quartic of genus one as trapped attractor.) This last example will study the case of a singular real quartic. As in [Bonifant and Dabija 02, Section 8.6], consider the Cassini quartic curve $\mathcal{C}$ with homogeneous equation $\Phi(x, y, z) = 0$, where[7]

$$\Phi(x, y, z) = \Phi_\kappa(x, y, z) = x^2y^2 - (x^2 + y^2)z^2 + \kappa z^4 \quad (7\text{–}1)$$

depends on a single parameter $\kappa \neq 0, 1$. Over the complex numbers, this is a rational curve with nodes at the two points $(1 : 0 : 0)$ and $(0 : 1 : 0)$. That is, the uniformizing map $\mathbb{C}/\Omega \to \mathcal{C} \subset \mathbb{P}^2(\mathbb{C})$ has transverse self-intersections at these two points. Define a one-parameter family of homogeneous polynomial maps from $\mathbb{C}^3$ to itself by the formula $F(x, y, z) = F_a(x, y, z) = (X, Y, Z)$, where

$$\begin{aligned} X &= -2xy(x^2 + y^2 - 2\kappa z^2), \\ Y &= y^4 - x^4, \\ Z &= -a\Phi(x, y, z) + 2xy(x^2 - y^2). \end{aligned} \quad (7\text{–}2)$$

[7]This expression yields curves that are equivalent, under a complex linear change of coordinates, to quartic curves introduced in 1680 by the French–Italian astronomer Giovanni Domenico Cassini, in connection with planetary orbits.

According to [Bonifant and Dabija 02], the curve $\mathcal{C}$ is invariant under the induced rational map $f = f_a : \mathbb{P}^2 \to \mathbb{P}^2$. It is not hard to check that the singular point $(0 : 1 : 0) \in \mathcal{C}$ (the "north pole" in Figures 13 and 14) is a saddle fixed point of f_a, with eigenvalues -2 and 0, and that the point $(0 : 0 : 1)$ (near the center of these figures) is a superattracting fixed point whenever $a \neq 0$.

If the parameters κ and a are real, then the corresponding real curve $\mathcal{C}(\mathbb{R}) = \mathcal{C} \cap \mathbb{P}^2(\mathbb{R})$ is connected when $\kappa < 0$, but has two connected components when $\kappa > 0$. These maps are illustrated in Figures 13 and 14 for the case $\kappa = \frac{1}{8} > 0$, with $\mathcal{C}(\mathbb{R})$ in black. Here the smaller component (which is nonsingular) maps to the larger invariant component $\mathcal{C}^0(\mathbb{R})$ (which has two singular points). Both branches of $\mathcal{C}^0(\mathbb{R})$ through the singular point $(1 : 0 : 0)$ map to just one of the two branches through the fixed point $(0 : 1 : 0)$, while both branches through $(0 : 1 : 0)$ map to the other branch through $(0 : 1 : 0)$. (All four branches lie within a single immersed circle that crosses itself twice within the nonorientable manifold $\mathbb{P}^2(\mathbb{R})$.) Note the identities

$$F(-x, -y, z) = F(x, y, z)$$

and

$$F^{\circ 2}(-y, x, z) = F^{\circ 2}(x, y, z)\,,$$

which imply that the Julia set of f_a has a 90° rotational symmetry, clearly visible in Figures 13 and 14. We will prove the following result.

Theorem 7.2. (A trapped attractor.) *If $0 < |\kappa| < \frac{1}{4}$ and if a is sufficiently small, then the invariant curve $\mathcal{C}^0(\mathbb{R})$ is a trapped attractor for the map f_a on the real projective plane that is induced by* (7–2).

Proof: Let $(X, Y, Z) = F(x, y, z)$. The quotient

$$\Phi_F(x, y, z) = \frac{\Phi(X, Y, Z)}{\Phi(x, y, z)}$$

is a polynomial of degree 12 in x, y, z, depending on the parameter a. In general, this polynomial seems rather complicated, but in the special case $a = 0$, computation shows that it takes the simple form

$$\Phi_F(x, y, z) = 16\kappa x^2y^2(x^2 - y^2)^4. \quad (7\text{–}3)$$

As a convenient measure of the distance of a point of $\mathbb{P}^2$ from the curve $\Phi = 0$ we take the ratio

$$r(x : y : z) = \frac{|\Phi(x, y, z)|}{(x^2 + y^2)^2}\,,$$

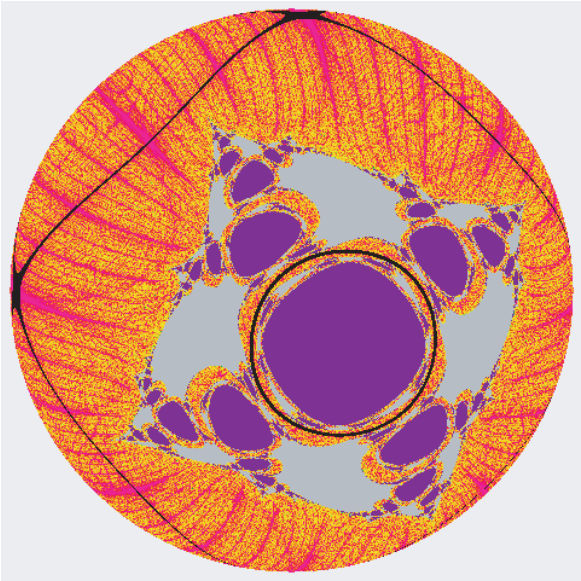

FIGURE 13. (See Example 7.1.) The Cassini quartic with parameter $k = \frac{1}{8}$, shown in black, consists of an outer circle $\mathcal{C}^0(\mathbb{R})$ with two self-intersections and a much smaller inner circle $\mathcal{C}^1(\mathbb{R})$. Here the warmer colors describe convergence toward $\mathcal{C}^0(\mathbb{R})$ for the rational map f_1 with parameter $a = 1$. The blue region is the basin of a superattracting fixed point at $(0 : 0 : 1)$, while the gray region is the basin of another attracting fixed point directly above it at $(0 : 1 : 2)$.

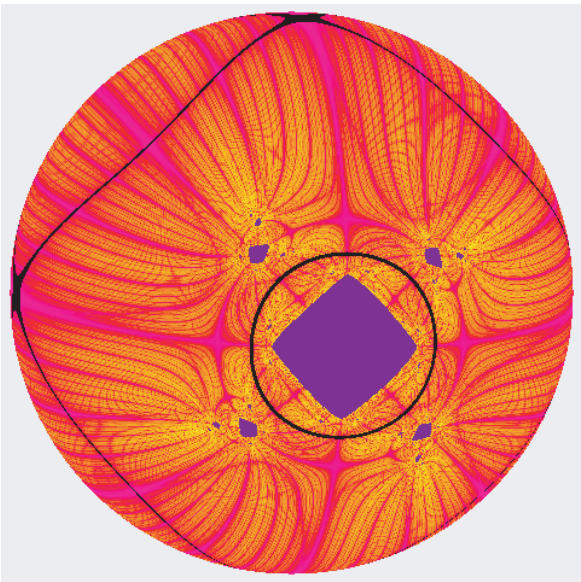

FIGURE 14. Corresponding picture for the same Cassini quartic with $k = \frac{1}{8}$, but using the map with parameter $a = \frac{2}{5}$.

with Φ as in (7–1). This ratio is well defined and finite except at the value $r(0:0:1) = +\infty$, and it vanishes only on the Cassini curve.

We want to prove an inequality of the form

$$r(X:Y:Z) \le \lambda r(x:y:z) \tag{7–4}$$

whenever $r(x:y:z)$ is sufficiently small, where $\lambda < 1$ is constant. To do this, we consider the ratio

$$r_f(x,y,z) = \frac{r(X:Y:Z)}{r(x:y:z)} = \left|\frac{\Phi(X,Y,Z)}{\Phi(x,y,z)}\right| \frac{(x^2+y^2)^2}{(X^2+Y^2)^2}.$$

In the special case $a = 0$, using the identity (7–3) and the inequality

$$X^2 + Y^2 \ge Y^2 = (y^4 - x^4)^2 = (x^2+y^2)^2(x^2-y^2)^2\,,$$

together with $|2xy| \le x^2 + y^2$, we see that

$$\begin{aligned}\frac{r(X:Y:Z)}{r(x:y:z)} &\le \left|\frac{\Phi(X,Y,Z)}{\Phi(x,y,z)}\right| \frac{(x^2+y^2)^2}{(x^2+y^2)^4(x^2-y^2)^4} \\ &= \frac{16|\kappa|x^2y^2}{(x^2+y^2)^2} \le 4|\kappa|.\end{aligned}$$

If $0 < |\kappa| < \frac{1}{4}$, then we can choose λ such that $4|\kappa| < \lambda < 1$. If N is any compact subset of $\mathbb{P}^2(\mathbb{R}) \smallsetminus \{(0:0:1)\}$, then for any a that is sufficiently close to zero, it follows by continuity that the required inequality (7–4) holds uniformly throughout N. Thus all orbits of f_a in N converge uniformly to the subset $\mathcal{C}(\mathbb{R})$. In the case that there are two components, the image $f_a(\mathcal{C}(\mathbb{R}))$ is necessarily equal to the component $\mathcal{C}^0(\mathbb{R}) \subset \mathcal{C}(\mathbb{R})$ that contains the fixed point $(0:1:0)$, and it follows that all orbits in N converge uniformly to $\mathcal{C}^0(\mathbb{R})$. □

Remark 7.3. (The case $a = 0$.) In the limiting case $a = 0$, there is no superattracting point, and in fact, $(0:0:1)$ becomes a point of indeterminacy. It follows easily from the argument above that the basin of $\mathcal{C}^0(\mathbb{R})$ under this limiting map f_0 is the entire domain of definition $\mathbb{P}^2(\mathbb{R}) \smallsetminus \{(0:0:1)\}$, provided that $0 < |\kappa| < \frac{1}{4}$.

The complex case is quite different, since a complex genus-one curve can never be a trapped attractor. The proof will occupy the rest of this section.

Theorem 7.4. (No complex trapping.) *Let $\mathcal{C} \subset \mathbb{P}^2 = \mathbb{P}^2(\mathbb{C})$ be a genus-one curve and let N be a neighborhood of $\mathcal{C}$. Then there cannot exist any holomorphic map $f : N \to N$ mapping $\mathcal{C}$ onto itself such that $\bigcap_n f^{\circ n}(N) = \mathcal{C}$.*

We first carry out the argument for an elliptic curve (necessarily of degree three), and then show how to modify the proof for a singular genus-one curve (necessarily of degree greater than three). The proof for a smooth $\mathcal{C}$ will be based on the following construction.

Definition 7.5. Let N_ϵ be the ϵ-neighborhood consisting of all points with distance less than ϵ from $\mathcal{C}$, using the standard Fubini–Study metric[8] on $\mathbb{P}^2$. If $\mathcal{C}$ is smooth and ϵ is sufficiently small, then N_ϵ is the total space of a real analytic fibration $\Pi : N_\epsilon \to \mathcal{C}$, where $\Pi(p)$ is defined to be the point $q \in \mathcal{C}$ that is closest to p. Furthermore, although this projection map Π is not holomorphic, each fiber $F_q = \Pi^{-1}(q)$ is a holomorphically embedded complex disk that is contained in the complex line orthogonal to $\mathcal{C}$ at q.

Lemma 7.6. (Curves in a neighborhood.) *With $\mathcal{C} \subset N_\epsilon$ as above, any nonconstant holomorphic map $\varphi : \mathcal{C}_1 \to N_\epsilon$ from an elliptic curve into N_ϵ must be an immersion, and must intersect each fiber F_q transversally, so that the composition $\Pi \circ \varphi$ is a real analytic immersion of $\mathcal{C}_1$ onto $\mathcal{C}$ of positive degree.*

In other words, $\mathcal{C}_1$ is a (real analytic) k-fold covering surface of $\mathcal{C}$, where $k \ge 1$ is the degree of $\Pi \circ \varphi$.

Proof of Lemma 7.6: Suppose to the contrary that there exists a critical point for the composition $\Pi \circ \varphi : \mathcal{C}_1 \to \mathcal{C}$. It will be convenient to rotate the coordinates for $\mathbb{P}^2$ as follows. Using (x,y) as an abbreviation for the point with coordinates $(x:y:1)$, we may assume that the critical value in $\mathcal{C} \subset \mathbb{P}^2$ has coordinates $(0,0)$ and that the tangent line to $\mathcal{C}$ at this critical value has equation $y = 0$. The fiber through this point is then a disk in the line $x = 0$. Choose a parametrization $t \mapsto \big(x(t), y(t)\big)$ for $\mathcal{C}$ such that $x(0) = y(0) = 0$, $y'(0) = 0$, and choose a parametrization $s \mapsto \big(x_1(s), y_1(s)\big)$ for $\varphi(\mathcal{C}_1)$ such that the critical point in $\mathcal{C}_1$ is $\big(x_1(0), y_1(0)\big) = (0, y_0)$, lying in the fiber $x = 0$. Now expand the function $x_1(s)$ as a power series

$$x_1(s) = cs^n + \text{ (higher-order terms)}\,,$$

with $c \ne 0$. Here $n \ge 2$, since otherwise $\varphi(\mathcal{C}_1)$ would cross the fiber $x = 0$ transversally.

[8] In terms of homogeneous coordinates $(x_0 : x_1 : \cdots : x_n)$ normalized so that $\sum |x_k|^2 = 1$, this metric takes the form $dt^2 = \sum |dx_k|^2 - |\sum \overline{x}_k\, dx_k)|^2$. With this normalization, the Riemannian distance $0 \le \theta \le \pi/2$ between two points $(x:y:z)$ and $(u:v:w)$ of $\mathbb{P}^2$ can be computed by the formula $\cos(\theta) = |\overline{x}u + \overline{y}v + \overline{z}w|$.

Using coordinates (x, y) for N_ϵ near the point $(0, 0)$ and using the parameter t for $\mathcal{C}$, we can think of the real analytic projection $\Pi : N_\epsilon \to \mathcal{C}$ as a correspondence $(x, y) \mapsto t = \widehat{t}(x, y)$. Setting $y = y_0 + \eta$, we can write the power series expansion for $\widehat{t}(x, y)$ at the point $(0, y_0) = \big(x_1(0), y_1(0)\big)$ as

$$\begin{aligned}\widehat{t}(x, y_0 + \eta) = x\big(a_1 + (a_2 x + a_3\overline{x} + a_4\eta + a_5\overline{\eta}) + \cdots\big) \\ + \overline{x}\big(b_1 + (b_2 x + b_3\overline{x} + b_4\eta + b_5\overline{\eta}) + \cdots\big),\end{aligned}$$

where the dots stand for terms of degree ≥ 2 in x, $\overline{x}$, η, and $\overline{\eta}$, and where the a_j and b_j are complex numbers with $|a_1| > |b_1|$, since the projection from (x, y_0) to its image in $\mathcal{C}$ must preserve orientation for x near 0. (Here we can assume that $b_2 = a_3$.) Therefore the composition $s \mapsto (x_1(s), y_1(s)) \mapsto \widehat{t}$ has power series

$$\widehat{t} = a_1 c\, s^n + b_1 \overline{c}\, \overline{s}^n + (\text{higher-order terms})\,.$$

This proves that the composition $\Pi \circ \varphi : \mathcal{C}_1 \to \mathcal{C}$ has an isolated critical point of local degree $n \geq 2$ (and hence multiplicity $n - 1 \geq 1$) at the point $s = 0$. Thus every critical point is isolated, and it follows that $\Pi \circ \varphi$ is a branched covering, with only finitely many critical points.

Although $\Pi \circ \varphi$ is not actually holomorphic, it behaves topologically just like a holomorphic map, so that we can apply the Riemann–Hurwitz theorem. (Compare Remark 2.2.) Thus the Euler characteristic $\chi(\mathcal{C}_1)$ is equal to $k\chi(\mathcal{C}) - \nu$, where k is the degree of $\Pi \circ \varphi$ and where ν is the number of critical points counted with multiplicity. Since $\chi(\mathcal{C}_1) = \chi(\mathcal{C}) = 0$, this proves that $\nu = 0$, as required. □

In particular, it follows easily that the composition $\Pi \circ \varphi : \mathcal{C}_1 \to \mathcal{C}$ is quasiconformal.

Definition 7.7. The *complex dilatation* of a C^1-smooth map $z \mapsto g(z)$ is the ratio

$$\mu_g(z) = \frac{\partial g/\partial \overline{z}}{\partial g/\partial z} \in \mathbb{C} \cup \infty\,.$$

Such a map is *quasiconformal*[9] if and only if $|\mu_g| < \text{constant} < 1$. (This absolute value is sometimes known as the "small dilatation" of g, while the ratio

$$K(z) = \frac{1 + |\mu_g|}{1 - |\mu_g|} \geq 1$$

is called the *dilatation*.)

[9] For general quasiconformal maps that need not be C^1-smooth, see [Ahlfors 66] or [Krushkal′ 79].

Now consider an infinite sequence of holomorphic immersions $\varphi_j : \mathcal{C}_j \to N_\epsilon$, where each $\mathcal{C}_j$ is a compact Riemann surface of genus one.

Lemma 7.8. (Converging quasiconformal maps.) *If the successive images $\varphi_j(\mathcal{C}_j)$ converge to $\mathcal{C}$ in the Hausdorff topology (or in other words, if the distance of each point of $\varphi_j(\mathcal{C}_j)$ from $\mathcal{C}$ converges uniformly to zero), then the complex dilatation of the quasiconformal map $\Pi \circ \varphi_j : \mathcal{C}_j \to \mathcal{C}$ converges uniformly to zero as $j \to \infty$.*

The proof of Lemma 7.8 will be based on the following preliminary statement, which is needed in order to control first derivatives.

Lemma 7.9. (Converging tangent spaces.) *With the φ_j as in Lemma 7.8, consider a sequence of points $\varphi_j(p_j) \in \varphi_j(\mathcal{C}_j)$ converging to a point $q \in \mathcal{C}$. Then the tangent space to $\varphi_j(\mathcal{C}_j)$ at $\varphi_j(p_j)$ converges to the tangent space to $\mathcal{C}$ at q. Furthermore, this convergence is uniform as we vary the points p_j and q.*

Proof: In fact, the argument will show that each branch of the curve $\varphi_j(\mathcal{C}_j)$ converges holomorphically to $\mathcal{C}$ throughout a neighborhood of q. As in the proof of Lemma 7.6, we can choose coordinates (x, y) such that $(0, 0)$ corresponds to the point q and such that the line $y = 0$ is tangent to $\mathcal{C}$ at q. Then the curve $\mathcal{C}$ is locally the graph of a holomorphic function $y = \psi_0(x)$.

We can fiber a neighborhood of $(0, 0)$ by a local projection into $\mathcal{C}$, mapping each (x, y) to the point $\Pi_0(x, y) = \big(x, \psi_0(x)\big) \in \mathcal{C}$. For any immersion $\varphi_j : \mathcal{C}_j \to \mathbb{P}^2$ with image in a small neighborhood of $\mathcal{C}$, we claim that the image of φ_j crosses the line $x = 0$ transversally near $(0, 0)$.

To prove this, we must smoothly interpolate between the projection $\Pi : N_\epsilon \to \mathcal{C}$ of Lemma 7.6, which is defined everywhere near $\mathcal{C}$, and the projection Π_0, which is well behaved only near $(0, 0)$. Using such a modified projection, which coincides with Π outside of a neighborhood of $(0, 0)$ and which coincides with Π_0 within a smaller neighborhood, the proof proceeds just as before.

Any branch of one of these approximating curves $\varphi_j(\mathcal{C}_j)$ near $(0, 0)$ can be described locally as the graph of a holomorphic function $y = \psi_j(x)$. Choosing a sequence of such branches that converge uniformly to ψ_0, it follows from a theorem of Weierstrass that every iterated derivative $d^k\psi_j(x)/dx^k$ converges uniformly to $d^k\psi_0(x)/dx^k$ throughout a slightly smaller neighborhood, as required. □

Proof of Lemma 7.8: With coordinates (x, y) as above, let $t \mapsto \big(x(t), y(t)\big)$ be a local parametrization of the curve $\mathcal{C}$ with $x(0) = y(0) = 0$, $y'(0) = 0$. It will be convenient to construct new local holomorphic coordinates (u, v) by the formula

$$(x, y) = \big(x(u), y(u) + v\big)\,.$$

In these new coordinates, the curve $\mathcal{C}$ has equation $v = 0$. The projection Π is then represented by a real analytic map $(u, v) \mapsto \hat{t}(u, v)$, where $\hat{t}(u, 0) = u$, so that $\partial\hat{t}/\partial u = 1$ and $\partial\hat{t}/\partial\overline{u} = 0$ when $v = 0$. For j large, we can choose $s = u$ as parameter for the nearby curve $\varphi_j(\mathcal{C}_j)$, so that the parametrization takes the form $s \mapsto \big(u_j(s), v_j(s)\big)$ with $u_j(s) = s$. For the composition $s \mapsto \hat{t}(s, v_j(s))$, it follows that

$$\frac{\partial\hat{t}}{\partial\overline{s}} = \frac{\partial\hat{t}}{\partial\overline{u}} + \frac{\partial\hat{t}}{\partial\overline{v}}\,\overline{dv_j/ds}\,,$$

where $\partial\hat{t}/\partial\overline{u}$ tends to zero as $v_j \to 0$ by the remarks above, and where dv_j/ds tends to zero as $v_j \to 0$ by Lemma 7.9. It follows easily that the complex dilatation

$$\mu_{\Pi\circ\varphi} = \frac{\partial\hat{t}/\partial\overline{s}}{\partial\hat{t}/\partial s}$$

tends to zero as $j \to \infty$, as required. □

Proof of Theorem 7.4 for an embedded curve: The proof will be based on the fact that any elliptic curve $\mathcal{C} \subset \mathbb{P}^2(\mathbb{C})$ can be approximated arbitrarily closely by other elliptic curves that are not conformally isomorphic to it. For example, after a linear change of coordinates, any such $\mathcal{C}$ is defined by an equation of the form $x^3+y^3+z^3 = 3\kappa xyz$, and by varying the parameter κ we can then find nearby curves that are not conformally isomorphic to $\mathcal{C}$.

Now assume that $\mathcal{C}$ is a trapped attractor. Let N_ϵ be a tubular neighborhood, as in Lemma 7.6. Then we can choose a trapping neighborhood $N_{\text{trap}} \subset N_\epsilon$ and then a smaller tubular neighborhood N_δ such that

$$\mathcal{C} \subset N_\delta \subset N_{\text{trap}} \subset N_\epsilon\,.$$

We will then construct a sequence of real analytic retractions $g_m : N_\delta \to \mathcal{C}$ of the form

$$g_m = f^{-m} \circ \Pi \circ f^{\circ m}\,.$$

More precisely, since f^{-m} is not uniquely defined, we will construct $g_m : N \to \mathcal{C}$ such that

$$f^{\circ m} \circ g_m = \Pi \circ f^{\circ m}\,,$$

with g_m equal to the identity map on $\mathcal{C}$. (Compare Figure 15. Here $\Pi : N_\epsilon \to \mathcal{C}$ is again the orthogonal projection that carries each $p \in N_\epsilon$ to the closest point of $\mathcal{C}$.)

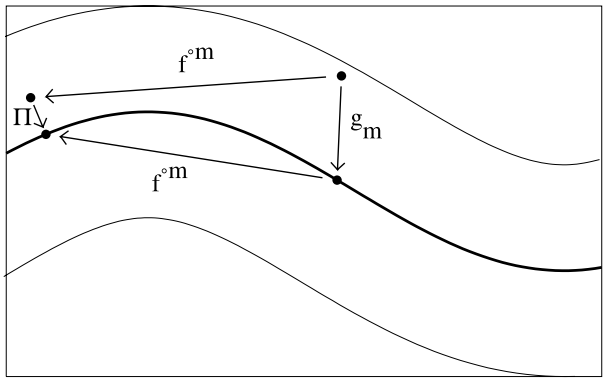

FIGURE 15. Construction of the retraction g_m from N_δ to $\mathcal{C}$.

To do this, let us first pass to the universal covering spaces $\widetilde{\mathcal{C}} \subset \widetilde{N}_\delta \subset \widetilde{N}_\epsilon$. (Since $\mathcal{C} \cong \mathbb{C}/\Omega$, it follows that $\widetilde{\mathcal{C}} \cong \mathbb{C}$.) Then f and Π lift to smooth maps

$$\widetilde{\mathcal{C}} \subset \widetilde{N}_\delta \xrightarrow{\widetilde{f}} \widetilde{N}_\epsilon \xrightarrow{\widetilde{\Pi}} \widetilde{\mathcal{C}}\,,$$

where we can choose the lift so that $\widetilde{\Pi}$ reduces to the identity map on $\widetilde{\mathcal{C}}$.

Since $\widetilde{f}$ is a linear map of $\widetilde{\mathcal{C}} \cong \mathbb{C}$, it follows that $\widetilde{f}^{-1}$ is well defined. Therefore the map

$$\widetilde{g}_m = \widetilde{f}^{-m} \circ \widetilde{\Pi} \circ \widetilde{f}^{\circ m} : \widetilde{N}_\delta \to \widetilde{\mathcal{C}}$$

is well defined, and it reduces to the identity map on $\widetilde{\mathcal{C}}$.

Finally, since $\widetilde{g}_m$ commutes with the group of deck transformations[10] of $\widetilde{N}_\delta$ over N_δ, it follows that $\widetilde{g}_m$ gives rise to a corresponding retraction $g_m : N_\delta \to \mathcal{C}$.

Let $\mathcal{C}' \subset N_\delta$ be a smoothly embedded elliptic curve that is not conformally equivalent to $\mathcal{C}$. Then it follows using Lemma 7.6 that each g_m maps $\mathcal{C}'$ diffeomorphically onto $\mathcal{C}$. Furthermore, since the successive images $f^{\circ m}(\mathcal{C}')$ must converge to $\mathcal{C}$, it follows from Lemma 7.8 that the complex dilatation of the immersion $\Pi \circ f^{\circ m} : \mathcal{C}' \to \mathcal{C}$ tends to zero as $h \to \infty$. Since $f^{\circ m}$ is locally biholomorphic on both $\mathcal{C}'$ and $\mathcal{C}$, this implies that the complex dilatation of $g_m : \mathcal{C}' \to \mathcal{C}$ also tends to zero as $h \to \infty$.

Thus, to complete the proof of Theorem 7.4, we need only note the following well-known statement from Teichmüller theory.

Lemma 7.10. (A conformal isomorphism criterion.) *Suppose that there exist quasiconformal homeomorphisms from the elliptic curve $\mathcal{C}_1$ to $\mathcal{C}_2$ with complex dilatation*

[10] On the other hand, the lifted map $\widetilde{f}$ does not commute with deck transformations. In fact, if G is the group of deck transformations, then f induces an embedding $f_* : G \to G$, with $\widetilde{f}(\sigma\widetilde{p}) = f_*(\sigma)\widetilde{f}(\widetilde{p})$ for each $\sigma \in G$.

arbitrarily close to zero. Then $\mathcal{C}_1$ must be conformally isomorphic to $\mathcal{C}_2$.

Proof: This is an immediate consequence of compactness of the space of quasiconformal homeomorphisms with bounded complex dilatation. On a more elementary level, if $\mathcal{C}_1 \cong \mathbb{C}/\Omega_1$ and $\mathcal{C}_2 \cong \mathbb{C}/\Omega_2$, where Ω_1 and Ω_2 are unimodular lattices, then the optimal quasiconformal map in any homotopy class is given by a real linear map corresponding to a linear transformation $L \in \mathrm{SL}(2,\mathbb{R})$ with $L(\Omega_1) = \Omega_2$. (Compare [Krushkal′ 79, p. 101].) Such a linear transformation has complex dilatation zero only if L is a rotation. Similarly, if a sequence of elements of $\mathrm{SL}(2,\mathbb{R})$ has complex dilatation converging to zero, then some subsequence must converge to a rotation, and the conclusion of Lemma 7.10 follows easily. □

This completes the proof of Theorem 7.4 for the case of an embedded curve. □

Proof in the singular case: Now consider a genus-one curve $\mathcal{C} \subset \mathbb{P}^2(\mathbb{C})$ with singular points (necessarily of degree four or more). Thus the uniformizing map $\iota : \mathbb{C}/\Omega \to \mathcal{C}$ must have either critical points or self-intersections or both. As usual, assume that $\mathcal{C}$ is invariant under a rational self-map f of $\mathbb{P}^2$. We will first prove the following preliminary statement.

Lemma 7.11. (The branches fold together.) *If $\mathcal{C}$ is a trapped attractor under some rational map f of $\mathbb{P}^2$, then the uniformizing map $\iota : \mathbb{C}/\Omega \to \mathcal{C}$ is necessarily an immersion. In particular, $\mathcal{C}$ cannot have any cusps. Furthermore, some iterate $f^{\circ n}$ must map all of the branches of $\mathcal{C}$ through any singular point p into a single branch through $f^{\circ n}(p)$.*

Proof: Recall that the map f restricted to $\mathcal{C}$ lifts to a linear map, which we will denote by $f^\sharp$, from $\mathbb{C}/\Omega$ to itself. First suppose that the uniformizing map ι has critical points in $\mathbb{C}/\Omega$. Since there can be only finitely many, and since the lifted map $f^\sharp$ must send critical points to critical points, it follows that there must be a periodic critical point. Thus replacing f and $f^\sharp$ by some iterate, we may assume that there is a fixed critical point. In terms of suitable local coordinates around this point and its image in $\mathbb{P}^2$, the map ι will have a power series expansion of the form

$$t \mapsto \big(x(t), y(t)\big) = (t^m + \cdots, t^n + \cdots)$$

with $m > n \geq 2$. Let λ be the multiplier of $f^\sharp$. Then the equation $\iota(\lambda\, t) = f\big(\iota(t)\big)$ implies that the eigenvalues of the derivative f' at the critical value are λ^m and λ^n. Since $|\lambda| > 1$, it follows that this critical value is a repelling fixed point for f, which contradicts the hypothesis that $\mathcal{C}$ has a trapping neighborhood.

Now suppose that we could find two branches through $\iota(t_1) = \iota(t_2) = p$ that map to distinct branches under all iterates of f. Since there are only finitely many singular points, these images must eventually cycle periodically. Thus, after replacing f by an iterate, we could find two distinct branches through some singular point q that both map to themselves. Since $f^\sharp$ has multiplier λ, it would follow easily that the eigenvalues of f' at q have the form λ and λ^m, where $m \geq 1$ is the intersection number between these two branches. Again this shows that q is a repelling point, contradicting the hypothesis that $\mathcal{C}$ has a trapping neighborhood. □

7.1 The Pulled-Back Neighborhood

For any small $\epsilon > 0$ we can "pull back" the ϵ-neighborhood $N_\epsilon = N_\epsilon(\mathcal{C})$ under the immersion ι to construct a formal neighborhood of $N_\epsilon^\sharp \supset \mathbb{C}/\Omega$. For each $t \in \mathbb{C}/\Omega$, let $D_\epsilon(t,\iota) \subset \mathbb{P}^2$ be the open unit disk in the line normal to $\iota(\mathbb{C}/\Omega)$ at $\iota(t)$, and let

$$N_\epsilon^\sharp = N_\epsilon^\sharp(\iota) \subset (\mathbb{C}/\Omega) \times \mathbb{P}^2$$

be the set of all pairs $(t,p) \in \mathbb{C}/\Omega \times \mathbb{P}^2$ with $t \in \mathbb{C}/\Omega$ and $p \in D_\epsilon(t,\iota)$. Then $N_\epsilon^\sharp$ is a real analytic manifold, and the projection $\Pi^\sharp(t,p) = t$ is a real analytic fibration of $N_\epsilon^\sharp$ over $\mathbb{C}/\Omega$. Furthermore, if ϵ is sufficiently small, then the projection $\widetilde{\iota}(t,p) = p$ will be a local diffeomorphism from $N_\epsilon^\sharp$ onto the open neighborhood $N_\epsilon \subset \mathbb{P}^2$. Using this local diffeomorphism $\widetilde{\iota}$, we can pull back the complex structure and make $N_\epsilon^\sharp$ into a complex manifold.

For the next lemma, we assume that f has been replaced by a suitable iterate $f^{\circ n}$, satisfying the conditions of Lemma 7.11.

Lemma 7.12. (Lifting the trapping neighborhood.) *If the singular curve $\mathcal{C}$ is a trapped attractor under some rational map f of $\mathbb{P}^2$ that folds branches together as in Lemma 7.11, then f lifts to a holomorphic map $f^\sharp$ from a neighborhood of $\mathbb{C}/\Omega$ in $N_\epsilon^\sharp$ into $N_\epsilon^\sharp$, with $\mathbb{C}/\Omega$ as trapped attractor.*

Proof: Given a pulled-back neighborhood $N_\epsilon^\sharp = N_\epsilon^\sharp(\iota)$ as above, by the uniform continuity of f on the compact set $\overline{N}_\epsilon(\mathcal{C})$, we can choose $\delta < \epsilon$ such that any curve of length $< \delta$ in $N_\epsilon(\mathcal{C})$ maps to a curve of length less than ϵ in $\mathbb{P}^2$. We can then form the neighborhood $N_\delta^\sharp(\iota) \subset$

$N_\epsilon^\sharp(\iota)$ of $\mathbb{C}/\Omega$, with image $\mathcal{C} \subset N_\delta(\mathcal{C}) \subset N_\epsilon(\mathcal{C})$, and with $f(N_\delta) \subset N_\epsilon$. We may also assume that δ is small enough that the projection that sends each point of N_δ to the closest point of $\mathcal{C}$ is uniquely defined, except within the ϵ-neighborhood of a branch point.

Now let $T \subset N_\delta$ be a trapping neighborhood for $\mathcal{C}$ and let $T^\sharp$ be the full preimage of T in $N_\epsilon^\sharp$. Then a lifted map $f^\sharp : T^\sharp \to T^\sharp$ can be constructed as follows. For each point $(t, p) \in T^\sharp \subset N_\epsilon^\sharp$ we can drop a perpendicular of length less than δ from p to some point $q \in \mathcal{C}$. The image under f will then be a curve of length less than ϵ joining $f(p)$ to $f(q) \in \mathcal{C}$. Deforming this curve to a minimal geodesic from $f(p)$ that meets $\mathcal{C}$ orthogonally, say at $\hat{q} = \iota(\hat{t})$, it follows that $(\hat{t}, f(p)) \in T^\sharp$, and we will set $f^\sharp(t, p) = (\hat{t}, f(p))$.

This construction does not appear to be well defined in the neighborhood of a singular point, since there may be perpendiculars of length less than δ from p to points on two or more branches of $\mathcal{C}$. However, by hypothesis these branches all map to a single branch of $\mathcal{C}$, so that the minimal geodesic from $f(p)$ to that branch of $\mathcal{C}$ is unique.

Finally, we must show that the intersection $A^\sharp$ of the iterated forward images of $T^\sharp$ is equal to $\mathbb{C}/\Omega$. Clearly, the projection from $T^\sharp$ onto T maps $A^\sharp$ onto $\mathcal{C}$. Therefore $A^\sharp$ is contained in the preimage of $\mathcal{C}$ in $T^\sharp$, which consists of $\mathcal{C}$, together with preimages of the ϵ-neighborhoods of the various branch points. (If $\iota(t_1) = \cdots = \iota(t_k)$, then there are $k - 1$ extra preimage branches through each of the points $t_1, \ldots, t_k$.) But $f^\sharp$ maps each of these extra branches back to $\mathbb{C}/\Omega$, so the attractor $A^\sharp$ is precisely $\mathbb{C}/\Omega$. □

The proof of Theorem 7.4 now proceeds just as in Lemmas 7.6 through 7.10 above. However, to carry out the argument in this new context, we must show that there are nearby curves that are not conformally isomorphic to $\mathbb{C}/\Omega$. In fact, we will prove the following, which will complete the proof.

Lemma 7.13. (Deforming immersed curves.) *Consider a Riemann surface of genus one of the form $\mathbb{C}/\Omega$, and let $F_\Omega : \mathbb{C}/\Omega \to \mathbb{P}^2$ be an immersion. Then for any small deformation Ω_t of the lattice Ω, we can construct a corresponding deformation F_{Ω_t} of the immersion F_Ω.*

Proof: Let $\widehat{\mathbb{P}}^2$ be the projective plane blown up at the three coordinate points $(1 : 0 : 0)$, $(0 : 1 : 0)$, and $(0 : 0 : 1)$. The following two statements are easily verified.

1. Any holomorphic immersion of a Riemann surface into $\mathbb{P}^2$ lifts uniquely to an immersion into $\widehat{\mathbb{P}}^2$, and any immersion into $\widehat{\mathbb{P}}^2$ projects to a map into $\mathbb{P}^2$ that is an immersion, except possibly over the three coordinate points.

   (The qualification is necessary, since, for example, the nonimmersion $t \mapsto (t^3 : t^2 : 1)$ from $\mathbb{P}^1$ into $\mathbb{P}^2$ lifts to an immersion into $\widehat{\mathbb{P}}^2$.)

2. We can construct a smooth embedding of $\widehat{\mathbb{P}}^2$ as a hypersurface in $\mathbb{P}^1 \times \mathbb{P}^1 \times \mathbb{P}^1$ by sending each $(x : y : z) \in \widehat{\mathbb{P}}^2$ to the triple (f, g, h), where $f = x/y$, $g = y/z$, $h = z/x$, with product $fgh = 1$.

The blowup guarantees, for example, that x/y makes sense, even at the point $(0 : 0 : 1)$. Interpreted in terms of local coordinates for $\mathbb{P}^1$, the equation $fgh = 1$ is well behaved, even when one or two of these functions take the value ∞. For example, near a point where $h = \infty$ but f and g are finite, we use h^{-1} as local coordinate, so that the equation takes the form $h^{-1} = fg$.

Thus to immerse a Riemann surface S into $\mathbb{P}^2$ we need only find three holomorphic functions f, g, h from S to $\mathbb{P}^1$ that yield an immersion of S into $\mathbb{P}^1 \times \mathbb{P}^1 \times \mathbb{P}^1$ and that have product equal to 1, taking care that nothing goes wrong over the three coordinate points. (The maps f, g, h need not have the same degree. For example, the functions $f(t) = g(t) = t$, $h(t) = 1/t^2$ from $\mathbb{P}^1$ to $\mathbb{P}^1$ yield the smooth quadratic variety $xz = y^2$.)

As noted above, F_Ω lifts to an embedding $t \mapsto \big(f(t), g(t), h(t)\big)$ of $\mathbb{C}/\Omega$ into the subset $\widehat{\mathbb{P}}^2 \subset \mathbb{P}^1 \times \mathbb{P}^1 \times \mathbb{P}^1$. Furthermore, each of the functions f and g can be expressed as a rational function of the Weierstrass function $\wp_\Omega(t)$ and its derivative $\wp'_\Omega(t)$. Choosing some explicit expressions for these rational functions and setting $h = 1/(fg)$, it follows that the map $t \mapsto \big(f(t), g(t), h(t)\big)$ deforms smoothly as we modify the lattice Ω. Evidently the requirement that this map project to an immersion into $\mathbb{P}^2$ will remain satisfied for all sufficiently small deformations. □

Lemma 7.13 having been proved, the proof of Theorem 7.4 is complete. □

8. HERMAN RINGS IN $\mathbb{P}^2$

In Example 5.5 we presented empirical evidence for the existence of a cycle of two attracting Herman rings for a substantial collection of complex Desboves maps with real coefficients. This section will explore what we can say more generally about Herman rings and Siegel disks

in $\mathbb{P}^2(\mathbb{C})$. (Compare Definition 1.2.) Note first that it is easy to construct special examples.

Example 8.1. (Rings contained in a complex line.) Let $(z_0 : z_1) \mapsto \big(p(z_0, z_1) : q(z_0, z_1)\big)$ be any degree-d rational map of $\mathbb{P}^1(\mathbb{C})$ that possesses a Herman ring. (For the existence of such rings, see Remark 8.11, and see for example [Shishikura 87].) Let $r(z_0, z_1, z_2)$ be any nonzero homogeneous polynomial of degree $d-1$. Then the map

$$f(z_0 : z_1 : z_2) = \big(p(z_0, z_1) : q(z_0, z_1) : z_2 r(z_0, z_1, z_2)\big)$$

of $\mathbb{P}^2(\mathbb{C})$ clearly has a Herman ring H that lies in the invariant line $z_2 = 0$. We can measure the extent to which this ring is attracting or repelling by using $\rho(z_0 : z_1 : z_2) = |z_2|/\sqrt{|z_0|^2 + |z_1|^2}$ as a measure of distance from the line $z_2 = 0$. If the ratio

$$\frac{\rho(f(z_0 : z_1 : z_2))}{\rho(z_0 : z_1 : z_2)} = |r| \sqrt{\frac{|z_0|^2 + |z_1|^2}{|p|^2 + |q|^2}}$$

is less than 1 everywhere on H, then this ring will be locally uniformly attracting, while if it is greater than 1 everywhere on H, then it will be locally uniformly repelling.

Thus we can always obtain an attracting H simply by multiplying any given $r(z_0, z_1, z_2)$ by a constant that is close to zero. Similarly, if $r(z_0 : z_1 : 0)$ is bounded away from zero throughout H, then we can obtain a repelling H by multiplying $r(z_0, z_1, z_2)$ by a large constant. In the first case, note that H will be contained in the Fatou set, while in the second case it will be contained in the Julia set. By choosing $r(z_0, z_1, z_2)$ more carefully, we can also find examples in which part of the ring is attracting and part is repelling. (Compare Lemmas 8.5 and 8.8.) The situation for attracting or repelling Siegel disks is completely analogous.

Example 8.2. (The Ueda construction.) Here is a quite different procedure, which yields a rich variety of dynamic behaviors. (Compare [Ueda 93] and [Fornæss 96, p. 13].) Recall that the n-fold *symmetric product* of $\mathbb{P}^1 = \mathbb{P}^1(\mathbb{C})$ with itself, that is, the quotient $(\mathbb{P}^1 \times \cdots \times \mathbb{P}^1)/S_n$ of the n-fold product by the symmetric group S_n of permutations of the n coordinates, can be naturally identified with $\mathbb{P}^n = \mathbb{P}^n(\mathbb{C})$. (This is proved by assigning to each homogeneous polynomial in two complex variables its collection of roots in $\mathbb{P}^1$.) Hence any rational map g of $\mathbb{P}^1$ gives rise to an everywhere-defined rational map $(g \times \cdots \times g)/S_n$ of $\mathbb{P}^n$. In particular, it gives rise to a map[11] $f = (g \times g)/S_2$ of $\mathbb{P}^2$. Now if U_1 and U_2 are disjoint invariant Fatou components in $\mathbb{P}^1$, then the product $U_1 \times U_2 \subset \mathbb{P}^1 \times \mathbb{P}^1$ can be identified with its image, which is an invariant Fatou component in $\mathbb{P}^2$. As examples:

- If $U_1 = H$ is a Herman ring in $\mathbb{P}^1$, and $U_2 = \mathcal{B}$ is the basin of an attracting fixed point, then $H \times \mathcal{B}$ is the basin of an attracting Herman ring in $\mathbb{P}^2$. Similarly, if S is a Siegel disk, then $S \times \mathcal{B}$ is the basin of an attracting Siegel disk.
- Furthermore, if H is a Herman ring in $\mathbb{P}^1$, and p is an arbitrary fixed point for the map g of $\mathbb{P}^1$, then $H \times \{p\}$ is a Herman ring for f. Since g has infinitely many repelling fixed points, it follows that f has infinitely many repelling Herman rings. Similarly, if g has a Siegel disk, then f has infinitely many repelling Siegel disks.
- If H and H' are disjoint Herman rings and S, S' are disjoint Siegel disks, then $H \times H'$, $H \times S$, and $S \times S'$ are three rotation domains in $\mathbb{P}^2$ with quite distinct topologies. (Compare the discussion of recurrent Fatou components in [Fornæss and Sibony 95a].)
- We can also give an example of a singular Siegel disk in $\mathbb{P}^2$. (Compare [Bedford and Smillie 91, p. 677].) Let S and S' be Siegel disks with rotation numbers $p\theta$ and $q\theta$, where $p, q > 1$ are relatively prime. In other words, suppose that we can choose parameters z and w for these disks such that z maps to $e^{2\pi i p\theta} z$ and w maps to $e^{2\pi i q\theta} w$ under g. Then the locus $z^q = w^p$ in $S \times S'$ is an invariant Siegel disk, embedded in this Siegel rotation domain, with a cusp singularity at the origin.

Remark 8.3. The construction described above can even be used to construct a Herman ring (or Siegel disk) in the *real* projective plane: Simply start with a rational map of $\mathbb{P}^1(\mathbb{C})$ with real coefficients that has two complex conjugate Herman rings (or Siegel disks), carry out the construction as described above, and then intersect with $\mathbb{P}^2(\mathbb{R})$.

8.1 The Transverse Lyapunov Exponent of a Ring or Disk

For any f-invariant Herman ring or Siegel disk, the transverse Lyapunov exponent is defined much as in the case

[11] More explicitly, if $g(x : y) = \big(p(x, y) : q(x, y)\big)$, then the map $f = (g \times g)/S_2$ can be described by the formula $f(x_1x_2 : x_1y_2 + y_1x_2 : y_1y_2) = (p_1p_2 : p_1q_2 + q_1p_2 : q_1q_2)$, where $p_j = p(x_j, y_j)$ and $q_j = q(x_j, y_j)$.

of an f-invariant elliptic curve, and this exponent is decisive as a test for attraction or repulsion. However, the transverse exponent for a ring or disk is no longer a constant, but is rather a real-valued function, constant on each invariant circle. Furthermore, it is piecewise linear and convex in terms of suitably chosen coordinates. To fix ideas, we will concentrate on the Herman ring case.

To begin the discussion, note that for any Herman ring $H \subset \mathbb{P}^2(\mathbb{C})$ (and more generally for any annulus) there is a conformal embedding $t : H \to \mathbb{C}/\mathbb{Z}$ that maps H isomorphically onto a cylinder of the form $h_0 < \Im(t) < h_1$ in $\mathbb{C}/\mathbb{Z}$. (This embedding is unique up to a translation or change of sign $t \mapsto \pm t +$ constant.) We will call t a *canonical parameter* on H. The difference $h_1 - h_0 > 0$ is called the *modulus* of H.

Lemma 8.4. (Holomorphic tubular neighborhoods.) *Let $\Gamma_h \subset H \subset \mathbb{P}^2$ be the invariant circle $\Im(t) = h$ contained in a Herman ring in the complex projective plane. Then we can parametrize some neighborhood $N = N(\Gamma_h)$ in $\mathbb{P}^2$ by holomorphic coordinates (t, u), where u ranges over a neighborhood of zero in $\mathbb{C}$, and t ranges over a neighborhood of the circle $\Im(t) = h$ in $\mathbb{C}/\mathbb{Z}$. Furthermore, these coordinates can be chosen such that t is the canonical parameter on $N \cap H$ and such that u is identically zero on this intersection.*

Proof: In the dual projective space consisting of all lines in $\mathbb{P}^2$, those lines that intersect Γ_h form a real 3-dimensional subset. Hence we can choose a line that misses Γ_h. After rotating the coordinates $(x : y : z)$, we may assume that this is the line $z = 0$. In other words, setting $X = x/z$, $Y = y/z$, we can introduce the affine coordinates $(X : Y : 1) = (x : y : z)$ throughout some neighborhood of Γ_h.

Let $X = X(t)$, $Y = Y(t)$ be the canonical parametrization of H throughout this neighborhood. Then the space of all unit vectors in $\mathbb{C}^2$ that are multiples of the tangent vector $\big(\dot{X}(t), \dot{Y}(t)\big)$ for some $\big(X(t), Y(t)\big) \in \Gamma_h$ has real dimension 2. Hence we can choose a fixed unit vector $\vec{V} \in \mathbb{C}^2$ that is not tangent to H at any point of Γ_h. The required coordinates (t, u) are now defined by the formula

$$(t,\, u) \mapsto \big(X(t),\, Y(t)\big) + u\,\vec{V}$$

for all $(t, u) \in (\mathbb{C}/\mathbb{Z}) \times \mathbb{C}$ with both $|\Im(t) - h|$ and $|u|$ sufficiently small. □

The map f, expressed in terms of these tubular coordinates in a neighborhood of Γ_h, has the form $(t, u) \mapsto (T, U)$, where $(t, 0)$ maps to $(t + \alpha, 0)$ for some irrational rotation number α. Evidently we can identify the transverse derivative along H_0 with the partial derivative

$$\frac{\partial U}{\partial u}\big(t, 0\big)\,.$$

The transverse Lyapunov exponent is then defined as the horizontal average

$$\mathrm{Lyap}(t) = \int_0^1 \log \left| \frac{\partial U}{\partial u}(t + \tau) \right| d\tau\,,$$

where we integrate over the interval $0 \le \tau \le 1$. If there are no zeros of $\partial U/\partial u$ in the strip $h_0 < \Im(t) < h_1$, $u = 0$, then $\mathrm{Lyap}(t)$ is an average of harmonic functions, and hence is harmonic. Since this harmonic function is constant on horizontal lines, it must be a *linear* function of the imaginary part $\Im(t)$. (We will sharpen this statement in Lemma 8.8.) The dynamical implications of this Lyapunov exponent can be described as follows.

Lemma 8.5. (Attraction or repulsion.) *If* $\mathrm{Lyap}(t)$ *is negative along the invariant circle $\Gamma_h \subset H$, then a neighborhood of Γ_h in the Herman ring H is uniformly attracting in the transverse direction, and hence is contained in the Fatou set of f. On the other hand, if* $\mathrm{Lyap}(t)$ *is positive, then Γ_h is contained in the Julia set.*

Remark 8.6. In the intermediate case in which $\mathrm{Lyap}(t)$ is identically zero near Γ_h, we do not have enough information to decide. In fact, using Ueda's construction (Example 8.2), we can find examples illustrating both possibilities. We can choose f such that a neighborhood of H, with its dynamics, is isomorphic to (Herman ring) × (Siegel disk) and hence belongs to the Fatou set. On the other hand, we can choose f such that H corresponds to (Herman ring) × (parabolic point), and hence belongs to the Julia set.

Proof of Lemma 8.5: Recall that the map f restricted to the ring H has the form $t \mapsto t + \alpha$, where the rotation number α is real and irrational. To simplify the notation, let us translate the canonical parameter t so that it takes real values (modulo one) on our invariant circle (so that $h = 0$). Following Hermann Weyl, for any continuous function $g : \mathbb{R}/\mathbb{Z} \to \mathbb{C}$, the successive averages

$$A_n g(t) = \frac{1}{n} \sum_{0 \le j < n} g(t + j\alpha)$$

converge uniformly to the integral $\int_{\mathbb{R}/\mathbb{Z}} g(t)\, dt$.

To prove this statement, note that it is easily verified in the special case that $g(t)$ is a trigonometric polynomial of the form $\sum_{|k|\le N} a_k e^{2\pi i k t}$. But any continuous g can be uniformly approximated by such a trigonometric polynomial. (This follows, for example, from the Stone–Weierstrass theorem.) The conclusion follows.

First suppose that the transverse derivative $\frac{\partial U}{\partial u}(t,0)$ has no zeros on $\mathbb{R}/\mathbb{Z}$, so that the function $t \mapsto g(t) = \log\left|\frac{\partial U}{\partial u}(t,0)\right|$ is finite-valued near $\mathbb{R}/\mathbb{Z}$. If the average Lyap(0) of g on $\mathbb{R}/\mathbb{Z}$ is strictly positive (or strictly negative), then we can choose an integer $n > 0$ such that $A_n g(t)$ is strictly positive (or negative) and bounded away from zero on $\mathbb{R}/\mathbb{Z}$, and hence throughout some neighborhood of $\mathbb{R}/\mathbb{Z}$ in $\mathbb{C}/\mathbb{Z}$. Now consider an orbit $(t_0,u_0) \mapsto (t_1,u_1) \mapsto \cdots \mapsto (t_n,u_n)$ near the given circle Γ_0. Note that

$$\lim_{u_0\to 0}\frac{u_n}{u_0} = \frac{\partial u_n}{\partial u_0}(t_0,0) = \prod_{0\le j<n}\frac{\partial u_{j+1}}{\partial u_j}(t_0+j\alpha,0) = \exp\big(nA_n g(t)\big)\,.$$

Taking the log absolute value of both sides, if $A_n g(t) < \log(c) < 0$ on $\mathbb{R}/\mathbb{Z}$, then $|\partial u_n/\partial u_0| < c^n < 1$ when $u_0 = 0$, and it follows easily that $|u_n| \le c^n |u_0|$ uniformly throughout a neighborhood of our invariant circle. This proves that some neighborhood H_0 in H is uniformly attracted to Γ_0.

Similarly, if $A_n g(t) > \log(c) > 0$, then a neighborhood is uniformly repelled, so that Γ_0 is contained in the Julia set.

Now suppose that the holomorphic function $t \mapsto \frac{\partial U}{\partial u}(t,0)$ has zeros along the real axis. If $\mathrm{Lyap}(0) < 0$, then we can replace $g(t)$ by the truncated function $g_\nu(t) = \max\{g(t),\nu\}$, where ν is some negative real constant. If ν is sufficiently negative, then the integral $\int_0^1 g_\nu(t)\,dt$ will still be negative. Hence we can choose n such that $A_n g(t) \le A_n g_\nu(t) < \log(c) < 0$, and it again follows that a neighborhood H_0 of Γ_0 is uniformly attracting.

In the case $\mathrm{Lyap}(0) > 0$, we cannot assert that a neighborhood is uniformly repelling when it contains zeros of $\partial U/\partial u$. However, such zeros are necessarily isolated. It is not hard to check that the function $t \mapsto \mathrm{Lyap}(\Im(t))$ is continuous, and hence is positive throughout a neighborhood. Since the Julia set of f is closed, we can at least conclude that Γ_0 is contained in the Julia set. □

Remark 8.7. Although a Herman ring may attract an open neighborhood, it is conjectured that its closure $\overline{H}$ can never be a trapped attractor. If H can be extended to a larger Herman ring H', then this statement is completely clear, since nearby points of H' cannot be attracted to $\overline{H}$. However, the case of a maximal Herman ring, with boundary ∂H necessarily contained in the Julia set, requires further study. The situation for Siegel disks is completely analogous.

Lemma 8.8. (Piecewise linearity.) *Let $H \subset \mathbb{P}^2$ be a Herman ring with canonical parameter $t \in \mathbb{C}/\mathbb{Z}$, where $h_0 < \Im(t) < h_1$. Then the function* $\mathrm{Lyap} : (h_0,h_1) \to \mathbb{R}$ *is convex and piecewise linear, with a jump in derivative at h if and only if the transverse derivative $\partial U/\partial u$ has a zero on the circle $\Im(t) = h$. In fact, the change in derivative at h is equal to 2π times the number of zeros of $\partial U/\partial u$ on this circle, counted with multiplicity.*

In particular, if there are points in H where the Lyapunov exponent is strictly negative, then it follows that they form a connected subring $H^{\mathrm{attr}} \subset H$.

Proof of Lemma 8.8: We will adapt a classical argument due to Jensen. (See, for example, [Milnor 06b, Appendix A].) It will be convenient to use the abbreviated notation $\varphi(t) = \partial U/\partial u$ for the transverse derivative evaluated at $(t,0)$, and $\varphi'(t)$ for its derivative. If φ has no zeros on the circle $\Im(t) = h$, then we can compute the derivative of the transverse Lyapunov exponent by differentiating under the integral sign. Setting $t = \tau + ih$, we have

$$\frac{\partial}{\partial h}\log|\varphi(t)| = \frac{\partial}{\partial h}\Re\big(\log\varphi(t)\big) = \Re\Big(\frac{d\log\varphi(t)}{dt}\frac{\partial t}{\partial h}\Big) = \Re\Big(\frac{\varphi'}{\varphi}i\Big)$$

and therefore

$$\mathrm{Lyap}'(h) = \frac{d}{dh}\int_0^1 \log|\varphi(\tau+ih)|\,d\tau = \Re\int_0^1 i\frac{\varphi'}{\varphi}d\tau\,,$$

where φ' and φ are evaluated at $t = \tau + ih$ for $0 \le \tau \le 1$ with h constant. Briefly, we can write

$$\mathrm{Lyap}'(h) = \Re\int_{[0,1]\times\{h\}} i\frac{d\varphi}{\varphi}\,.$$

Given two numbers $h_0 < h_1$ such that φ has no zeros at height h_0 or h_1, we can now compute the difference $\mathrm{Lyap}'(h_1) - \mathrm{Lyap}'(h_0)$ as follows. Translating the parameter t horizontally if necessary, we may assume also that φ has no zeros on the vertical line $\Re(t) = 0$. Let R be the rectangle consisting of all $t \in \mathbb{C}$ with $0 \le \Re(t) \le 1$ and $h_0 \le \Im(t) \le h_1$. Integrating in the positive direction

around the boundary of R, since the integrals around the left and right sides cancel out, we obtain

$$\mathrm{Lyap}'(h_0) - \mathrm{Lyap}'(h_1) = \Re \oint_{\partial R} i\,\frac{d\varphi}{\varphi}\,.$$

But the integral $\oint_{\partial R} d\varphi/\varphi$ is equal to $2\pi i N(R)$, where $N(R)$ is the number of zeros of φ in R, so this equation reduces to $\mathrm{Lyap}'(h_1) - \mathrm{Lyap}'(h_0) = 2\pi N(R)$. This proves Lemma 8.8. □

Remark 8.9. (Siegel disks and punctured Siegel disks.) Let $\mathbb{D}\smallsetminus\{0\}$ be the open set consisting of all $z \in \mathbb{C}$ with $0 < |z| < 1$. By a *punctured Siegel disk* we mean a holomorphic embedding of $\mathbb{D}\smallsetminus\{0\}$ as an f-invariant subset of $\mathbb{P}^2$, mapped to itself by an irrational rotation.[12] The argument above shows that the transverse Lyapunov exponent of such a punctured disk can be expressed as a convex piecewise linear function of $\log(r)$, where $r = |z|$. Furthermore, since this transverse exponent is bounded from above, it must have the form $\mathrm{Lyap} = a\log(r) + b$ for small r, with $a \geq 0$. In particular, the set of points with $\mathrm{Lyap} < 0$ (if there are any) must be a punctured subdisk, corresponding to the set of z with $0 < |z| <$ constant.

In the case of a full Siegel disk with no puncture, we can supplement this discussion with the explicit formula

$$\frac{d\mathrm{Lyap}}{d\log(r)} = N(\mathbb{D}_r) \geq 0\,,$$

where $N(\mathbb{D}_r)$ is the number of zeros of the transverse derivative, counted with multiplicity, in the disk of radius r. This is essentially just a statement of Jensen's original computation. (See, for example, [Milnor 06b, p. 219].)

8.2 Herman Rings for Maps with Real Coefficients

Most known examples of Herman rings have been specially constructed. The surprise in Example 5.5 was to find an apparent example that appeared out of the blue, with no obvious reason to expect it. The set of complex rational maps of specified degree with a Herman ring presumably has measure zero, so that a randomly chosen example will never have a Herman ring. However, if we consider rational maps with real coefficients, then the situation is different, and the discussion in Example 5.5 suggests that the set of real parameters that give rise to a complex Herman ring should have positive Lebesgue measure.

[12] One example of a punctured Siegel disk that cannot be extended to a full smoothly embedded disk is described in Example 8.2 above. We don't know whether more-exotic examples exist.

Let f be a rational map of $\mathbb{P}^2$ with real coefficients, and suppose that there exists an embedded f-invariant circle $\Gamma \subset \mathbb{P}^2(\mathbb{R})$ with irrational rotation number. If Γ is smooth of class C^2, then according to Denjoy's theorem, the restriction $f|_\Gamma$ is topologically conjugate to a circle rotation. In particular, there is a canonical f-invariant probability measure $d\mu$ with support equal to the entire circle. The transverse Lyapunov exponent of Γ in $\mathbb{P}^2(\mathbb{R})$ is then well defined. Just as in the proof of Lemma 8.5, a positive Lyapunov exponent implies that Γ is uniformly repelling, and similarly, a negative exponent implies that Γ is uniformly attracting and hence is a trapped attractor.

In the real analytic case we can complexify the circle Γ to obtain the following.

Lemma 8.10. (From circle to ring.) *Let f be a rational map of $\mathbb{P}^2(\mathbb{R})$. If Γ is a real analytic f-invariant circle with Diophantine rotation number, then the associated map from $\mathbb{P}^2(\mathbb{C})$ to itself possesses a Herman ring $H \supset \Gamma$. Furthermore, the transverse Lyapunov exponent of Γ in $\mathbb{P}^2(\mathbb{R})$ is identical to the transverse Lyapunov exponent of H along Γ.*

If we exclude the special case that the transverse exponent is exactly zero, then it follows that Γ is repelling (or attracting) in the real projective plane if and only if a neighborhood of Γ in H is repelling (or attracting) in the complex projective plane.

Remark 8.11. (The one-dimensional case.) It is interesting to compare the situation in one variable. For any odd number $d \geq 3$, the set of degree-d rational maps that carry the real projective line $\mathbb{P}^1(\mathbb{R})$ diffeomorphically onto itself is open, and all possible rotation numbers are realized. If such a map has Diophantine rotation number, then a similar argument shows that the corresponding rational map of $\mathbb{P}^1(\mathbb{C})$ contains a Herman ring.

Proof of Lemma 8.10: By a theorem of Herman, as sharpened by Yoccoz (see [Yoccoz 02]), any orientation-preserving real analytic diffeomorphism of a circle with Diophantine rotation number α is real analytically conjugate to the rigid rotation $t \mapsto t+\alpha (\mathrm{mod}\mathbb{Z})$ of the standard circle $\mathbb{R}/\mathbb{Z}$. That is, there is a real analytic diffeomorphism $h : \mathbb{R}/\mathbb{Z} \to \Gamma \subset \mathbb{P}^2(\mathbb{R})$ such that $f(h(t)) = h(t+\alpha)$.

Since h is real analytic, it extends to a complex analytic diffeomorphism from a neighborhood of $\mathbb{R}/\mathbb{Z}$ in the cylinder $\mathbb{C}/\mathbb{Z}$ into the complex projective plane. The image of this extended map on some neighborhood

$\{t \mod \mathbb{Z} : |\Im(t)| < \epsilon\}$ is the required Herman ring $H \subset \mathbb{P}^2(\mathbb{C})$. Evidently the translation $t \mapsto t + \alpha$ on this neighborhood is conjugate to the rational map f on H. Further details are straightforward, since any norm on the normal bundle of H in $\mathbb{P}^2(\mathbb{C})$ will restrict to a norm on the normal bundle of Γ in $\mathbb{P}^2(\mathbb{R})$. □

Now consider a C^∞ smoothly embedded circle Γ_0 in a real 2-dimensional manifold M. Let $M \xrightarrow{f_0} M$ be a C^∞ smooth map that restricts to an irrational rotation on Γ_0 and that has negative transverse exponent on Γ_0. As noted above, an argument similar to the proof of Lemma 8.5 shows that Γ_0 is a trapped attractor. Let $N \subset M$ be a trapping neighborhood, with $f_0(N) \subset \text{interior}(N)$.

Theorem 8.12. (Persistence of invariant circles.) *In this situation, for any C^∞ map f_τ that is close enough to f_0 in the C^1 topology, the intersection*

$$\Gamma_\tau = \bigcap_n f_\tau^{\circ n}(N)$$

of the iterated forward images of N under f_τ will be a topological circle, and f_τ will map this circle homeomorphically onto itself with a rotation number ρ_τ that varies continuously with τ. Furthermore, for any finite k, if f_τ is C^1 sufficiently close to f_0, then Γ_τ will be C^k smooth.

Here we can expect the continuous function $\tau \mapsto \rho_\tau$ to have an interval of constancy whenever ρ_τ takes a rational value. In fact, a generic map f_τ with $\rho_\tau = p/q$ will have an attracting period-q orbit contained in Γ_τ. In this case, Γ_τ cannot contain any dense orbit. Evidently such an attracting orbit will be stable under perturbation.

Proof of Theorem 8.12: If a neighborhood of Γ_0 is orientable, then we can choose local coordinates (t, u) throughout some neighborhood of Γ_0, with $t \in \mathbb{R}/\mathbb{Z}$ and with $|u| < \epsilon$, so that Γ_0 is given by the equation $u = 0$, and so that the map f_0, in these coordinates, has the form

$$(t, u) \mapsto (T, U), \quad \text{where } (t, 0) \mapsto (t + \rho_0, 0)\,,$$

and where the rotation number ρ_0 is an irrational constant. Thus $T = t + \rho_0$ and $U = 0$ when $u = 0$. (In the nonorientable case, we can first pass to the 2-fold orientable covering of a neighborhood and then choose such coordinates.) Evidently $\partial T/\partial t = 1$ and $\partial U/\partial t = 0$ along the circle $u = 0$. Furthermore, since the transverse exponent is negative, after replacing f_0 by some high iterate, we may assume that $|\partial U/\partial u| < c$ when $u = 0$, for some constant $c < 1$.

After a carefully chosen change of coordinate, replacing (t, u) by $(\widehat{t}, \widehat{u})$, we will show that the corresponding map $(\widehat{t}, \widehat{u}) \mapsto (\widehat{T}, \widehat{U})$ satisfies the additional condition that $\partial\widehat{T}/\partial\widehat{u} = 0$ when $\widehat{u} = 0$. Let $\widehat{t} = t + \psi(t)u$, $\widehat{u} = u$, and correspondingly, $\widehat{T} = T + \psi(T)U$, $\widehat{U} = U$, where the auxiliary function ψ will be chosen below.

Along the line $u = U = 0$, we then have

$$d\widehat{T} = \frac{\partial\widehat{T}}{\partial\widehat{t}}\,d\widehat{t} + \frac{\partial\widehat{T}}{\partial\widehat{u}}\,d\widehat{u} = \frac{\partial\widehat{T}}{\partial\widehat{t}}\big(dt + \psi(t)du\big) + \frac{\partial\widehat{T}}{\partial\widehat{u}}\,du\,,$$

but also

$$d\widehat{T} = dT + \psi(T)dU = dt + \frac{\partial T}{\partial u}du + \psi(T)\frac{\partial U}{\partial u}\,du\,.$$

Combining these two equations with the required identity $\partial\widehat{T}/\partial\widehat{u} = 0$, we obtain

$$\psi(t) = \frac{\partial T}{\partial u}(t, 0) + \psi(t + \rho_0)\frac{\partial U}{\partial u}(t, 0)\,.$$

This difference equation can be solved by setting

$$\psi(t) = s_0 + r_0 s_1 + r_0 r_1 s_2 + \cdots\,,$$

where

$$s_n = \frac{\partial T}{\partial u}(t + n\rho_0, 0) \quad \text{and} \quad r_n = \frac{\partial U}{\partial u}(t + n\rho_0, 0)\,.$$

Since this series evidently converges uniformly, we obtain the required change of coordinates.

Henceforth, we will leave off the hats and simply assume that we have chosen coordinates such that $(t, u) \mapsto (T, U)$ with

$$\begin{aligned} \partial T/\partial t = 1, &\quad \partial U/\partial t = 0,\\ \partial T/\partial u = 0, &\quad |\partial U/\partial u| < c \end{aligned}$$

along the circle $u = U = 0$.

Next, given any $0 < \eta < 1$, we can choose a trapping neighborhood $N = \{(t, u); |u| \le b_0\}$ for Γ_0 that is small enough so that the inequalities

$$\begin{aligned} |\partial_t T - 1| < \eta, &\quad |\partial_u T| < \eta,\\ |\partial_t U| < \eta, &\quad |\partial_u U| < c, \end{aligned} \tag{8–1}$$

are valid throughout this neighborhood (using an abbreviated notation for partial derivatives). We can then choose f_τ close enough to f_0 that $f_\tau(N) \subset \text{interior}(N)$, so that these inequalities (8–1) remain true for the map $f_\tau(t, u) = (T, U)$.

Now consider a curve $t \mapsto u(t)$ with slope $v(t) = du/dt$. Setting $f_\tau\big(t, u(t)\big) = (T, U)$, we have

$$\frac{d\,T\big(t, u(t)\big)}{dt} = \frac{\partial T}{\partial t} + \frac{du}{dt}\frac{\partial T}{\partial u},$$

or briefly,

$$D_tT = \big(\partial_t + v\partial_u\big)T\,,$$

and similarly $D_tU = \big(\partial_t + v\partial_u\big)U$. Given some upper bound b_1 for $|v| = |du/dt|$, we can estimate that

$$D_tT > 1 - \eta - b_1\eta \qquad \text{and} \qquad |D_tU| < \eta + b_1 c\,,$$

and hence

$$\left|\frac{dU}{dT}\right| = \frac{|D_tU|}{D_tT} < \frac{\eta + b_1 c}{1 - \eta - b_1\eta}\,.$$

If η is sufficiently small, then this upper bound will be strictly less than b_1. More precisely, if

$$0 < \eta < \frac{b_1(1-c)}{1 + b_1 + b_1^2},$$

then a brief computation shows that $D_tT > 0$ and that $(\eta + b_1 c)/(1 - \eta - b_1\eta) < b_1$. It will then follow that the image curve is the graph of a well-defined function $U = U(T)$, and furthermore that the slope of this image curve is bounded by the same constant,

$$|dU/dT| < b_1\,.$$

It follows inductively that each iterated forward image of the initial curve will again be a well-defined curve with $|\text{slope}| < b_1$.

As trapping neighborhood N we can choose a union of horizontal circles $u = \hat{u}$ with $-b_0 \le \hat{u} \le b_0$. Then each iterated image $f_\tau^{\circ n}(N) \subset N$ will be a corresponding union of a continuum of curves of the form $u_n = u_n(t)$ with $|du_n/dt| \le b_1$. If $u_n^-(t)$ is the infimum of this collection of curves and $u_n^+(t)$ is the supremum, then it follows easily that the nth forward image of N is given by

$$f_\tau^{\circ n}(N) = \{(t,u) : u_n^-(t) \le u \le u_n^+(t)\}.$$

Here both the upper and lower boundary curves satisfy a Lipschitz condition

$$|u_n^\pm(t_1) - u_n^\pm(t_0)| \le b_1|t_1 - t_0|.$$

On the other hand, it follows from (8–1) that the Jacobian determinant of f_τ within N is bounded by

$$|\text{Jacobian}| < (1+\eta)c + \eta^2\,,$$

and we may assume that this upper bound is strictly less than one. Hence the areas of these successive images shrink to zero. Thus $\int_0^1 \big(u_n^+(t) - u_n^-(t)\big)\,dt$ tends to zero as $n \to \infty$. It follows easily that the upper and lower bounding curves tend to a common Lipschitz limit. This proves that the attracting set

$$\Gamma_\tau = \bigcap_{n\ge 0} f_\tau^{\circ n}(N)$$

is itself the graph of a function $t \mapsto \lim_{n\to\infty} u_n^\pm(t)$ that is continuous (and in fact Lipschitz with Lipschitz constant b_1).

Note that the rotation number ρ_τ of such a continuously varying family of monotone circle maps depends continuously on the parameter τ. (See [de Melo and van Strien 93, p. 33].)

To prove that this attracting curve is C^1 smooth, we must estimate second derivatives. It will be convenient to set

$$D_{t,t} = \partial_t^2 + 2v\partial_t\partial_u + v^2\partial_u^2 + (dv/dt)\partial_u,$$

so that

$$\frac{d^2U}{dt^2} = D_{t,t}U \quad \text{and} \quad \frac{d^2T}{dt^2} = D_{t,t}T\,.$$

Since $dU/dT = D_tU/D_tT$, it follows that

$$\begin{aligned}\frac{d^2U}{dT^2} &= \frac{d}{dT}\frac{D_tU}{D_tT} = \frac{D_t(D_tU/D_tT)}{D_tT}\\ &= \frac{(D_{t,t}U)(D_tT) - (D_{t,t}T)(D_tU)}{(D_tT)^3}\,.\end{aligned}$$

Separating out the $dv/dt = d^2u/dt^2$ terms, we can write this as

$$\frac{d^2U}{dT^2} = A_2 + B_2\frac{d^2u}{dt^2}\,, \tag{8–2}$$

where A_2 is uniformly bounded and where

$$B_2 = \frac{(\partial_uU)(D_tT) - (\partial_uT)(D_tU)}{(D_tT)^3}\,,$$

so that

$$|B_2| < \frac{c\,(1-\eta-b_1\eta) + \eta(\eta + b_1 c)}{(1-\eta-b_1\eta)^3}\,.$$

Evidently, if η is small enough, then $|B_2| < \text{constant} < 1$. Now choose a constant $b_2 > |A_2|/(1 - |B_2|)$. Then if $|d^2u/dt^2| < b_2$, it follows that

$$|d^2U/dT^2| < |A_2| + |B_2|b_2 < b_2\,.$$

Thus with these choices, the successive forward images of Γ_0 will be curves $u_n = u_n(t)$ that converge uniformly to a limit, with both $|du_n/dt|$ and $|d^2u_n/dt^2|$ uniformly bounded.

Now we can continue inductively. By successively differentiating the formula (8–2), we obtain formulas of the form

$$\frac{d^k U}{dT^k} = A_k + B_k \frac{d^k u}{dt^k},$$

where A_k depends not only on the iterated partial derivatives of $T(t,u)$ and $U(t,u)$ but also on the derivatives $d^\ell u/dt^\ell$ with $\ell < k$, and where

$$B_{k+1} = \frac{B_k}{D_t T} < \frac{B_k}{1-\eta-b_1\eta}.$$

Thus, choosing η small enough that $B_k < \text{constant} < 1$, we can find a suitable upper bound b_k for $|d^k u/dt^k|$ that is preserved when we replace a curve Γ by $f_\tau(\Gamma)$. Thus, given any finite k, we can choose η small enough that the iterated forward images of a curve $u = u(t)$ that satisfies the inequalities

$$\left|\frac{d^\ell u}{dt^\ell}\right| \le b_\ell \quad \text{for all } \ell \le k$$

will be a curve that satisfies these same inequalities.

To complete the proof of Theorem 8.12, we need the following lemma.

Lemma 8.13. (A derivative inequality.) *If a C^2 smooth function $x = x(t)$ on the real line satisfies uniform inequalities $|x(t)| < \alpha$ and $|d^2x/dt^2| < \beta$, then it follows that*

$$\left|\frac{dx}{dt}\right| < \sqrt{2\alpha\beta}.$$

Proof: Suppose, for example, that the first derivative $x' = dx/dt$ satisfied $x'(0) \ge \sqrt{2\rho_0\beta}$ with $x(0) \ge 0$. Using the lower bound $x''(t) > -\beta$ and integrating twice, we see that

$$x'(t) > \sqrt{2\alpha\beta} - \beta t \quad \text{and} \quad x(t) > \sqrt{2\alpha\beta}\,t - \beta t^2/2$$

for $t > 0$. In particular, substituting $t_0 = \sqrt{2\alpha/\beta}$, it would follow that $x(t_0) > \alpha$, thus contradicting the hypothesis. Other cases can be handled similarly. □

We can now complete the proof of Theorem 8.12. Again let $u_n = u_n(t)$ be the nth forward image of Γ_0 under f_τ. As m and n tend to infinity, the difference $u_n(t) - u_m(t)$ tends to zero, while the difference $u_n''(t) - u_m''(t)$ remains uniformly bounded. Thus it follows from Lemma 8.13 that the difference $u_n'(t) - u_m'(t)$ converges uniformly to zero.

Similarly, since differences of higher derivatives remain uniformly bounded, it follows inductively that differences of higher derivatives converge to zero. Thus, for any specified $k < \infty$, it follows that the limit curve Γ_τ is C^k smooth whenever τ is sufficiently close to zero. This completes the proof. □

Remark 8.14. Note that the argument above does not produce a C^∞ curve, since we need to impose tighter and tighter restrictions on f_τ in order to get successive higher derivatives. The argument certainly does not produce a real analytic curve, which is what we would need in order to show that Γ_τ is contained in a Herman ring. We have no idea how to prove real analyticity, even assuming that the rotation number ρ_τ is Diophantine.[13]

9. OPEN PROBLEMS

The results of this note leave a number of conjectures and open questions. Here is a brief list.

Conjecture 9.1. *For any f-invariant elliptic curve $\mathcal{C} \subset \mathbb{P}^2(\mathbb{C})$, the basin of attraction, consisting of all points whose orbits converge to $\mathcal{C}$, is contained in the Julia set of f.*

Intuitive proof: Otherwise the basin would have to contain an open set U such that every sequence of iterates of f on U contains a subsequence converging to a constant $c \in \mathcal{C}$. This looks very unlikely, given the fact that f is highly expanding in directions tangent to $\mathcal{C}$.)

The following two conjectures are closely related. Compare the discussion in Remark 4.3.

Conjecture 9.2. *Such an attracting basin cannot contain any nonvacuous open set. In other words, the set of all points not attracted to $\mathcal{C}$ is always everywhere dense.*

Conjecture 9.3. *Every invariant complex elliptic curve contains a repelling periodic point.*

In all examples known to us there is a repelling fixed point.

Conjecture 9.4. *In the space of complex Desboves maps with real coefficients, there is a subset of positive measure*

[13] In order to illustrate the difficulty of understanding simple closed curves, it is interesting to compare the boundaries of Siegel disks for rational maps of $\mathbb{P}^1$. These are simple closed curves in all known cases. They can never be real analytic, but in the non-Diophantine case they can be C^∞ smooth. (Compare [Avila et al. 04].) In the Diophantine case, such a boundary necessarily contains a critical point, and hence cannot be smooth. (See [Ghys 84].)

consisting of maps that have a cycle of attracting Herman rings.

(Compare Section 8 and Example 5.5.)

There are also many questions about which we have no idea what to guess.

- To what extent are maps with an attracting periodic orbit common in the space of all degree-d maps preserving a given elliptic curve? For example, do they form a dense open set?

- Can an invariant elliptic curve be a global attractor, with an attracting basin of full measure? We have constructed a number of examples in which this seems to be true empirically; but how can one exclude the possibility of other attractors with basins of very small measure?

- Can a smooth real elliptic curve be a trapped attractor?

- What can one say about the dynamics when the elliptic curve has positive transverse Lyapunov exponent? Could such a map have an absolutely continuous invariant measure? Is it true that an elliptic curve can never be a measure-theoretic attractor when its transverse exponent is positive? (Compare Remarks 1.4 and 6.8.)

- What other kinds of attractor can occur for a rational map with invariant elliptic curve? Can there be fractal attractors? Can there be a set of dense orbits of positive measure, or even of full measure? Can the Julia set have positive measure?

ACKNOWLEDGMENTS

We want to thank the National Science Foundation (DMS 0103646) and the Clay Mathematics Institute for their support of dynamical systems activities at Stony Brook.

We want to acknowledge the contribution of our coauthor Marius Dabija who died on June 22, 2003 before this paper was submitted for publication.

REFERENCES

[Ahlfors 66] L. V. Ahlfors. *Lectures on Quasiconformal Mappings*. Princeton: Van Nostrand, 1966.

[Alexander et al. 92] J. C. Alexander, I. Kan, J. Yorke, and Z. You. "Riddled Basins." *Int. J. Bifurcation and Chaos* 2 (1992), 795–813.

[Artebani and Dolgachev 06] M. Artebani and I. Dolgachev. "The Hesse Pencil of Plane Cubic Curves." arXiv:math.AG/0611590, 2006.

[Ashwin et al. 96] P. Ashwin, J. Buescu, and I. Stewart. "From Attractor to Chaotic Saddle: A Tale of Transverse Instability." *Nonlinearity* 9 (1996), 703–737.

[Ashwin et al. 98] P. Ashwin, P. Aston, and M. Nicol. "On the Unfolding of a Blowout Bifurcation." *Physica D* 111 (1998), 81–95.

[Auslander et al. 64] J. Auslander, N. P. Bhatia, and P. Seibert. "Attractors in Dynamical Systems." *Bol. Soc. Mat. Mexicana (2)* 9 (1964), 55–66.

[Avila et al. 04] A. Avila, X. Buff, and A. Cheritat. "Siegel Disks with Smooth Boundaries." *Acta Math.* 193 (2004), 1–30.

[Bedford and Smillie 91] E. Bedford and J. Smillie. "Polynomial Diffeomorphisms of $\mathbb{C}^2$. II: Stable Manifolds and Recurrence." *J. Amer. Math. Soc.* 4:4 (1991), 657–679.

[Bonifant and Dabija 02] A. Bonifant and M. Dabija. "Self-Maps of $\mathbb{P}^2$ with Invariant Elliptic Curves." In *Complex Manifolds and Hyperbolic Geometry (Guanajuato, 2001)*, pp. 1–25, Contemp. Math. 311. Providence, RI: Amer. Math. Soc., 2002.

[Briend and Duval 99] J.-Y. Briend and J. Duval. "Exposants de Lyapounoff et distribution des points périodiques répulsifs d'un endomorphisme de $\mathbb{CP}^k$." *Acta Math.* 182 (1999), 143–157.

[Briend and Duval 01] J.-Y. Briend and J. Duval. "Deux caractérisations de la mesure d'équilibre d'un endomorphisme de $\mathbb{P}^k(\mathbb{C})$." *Publ. Math. Inst. Hautes Études Sci.* 93 (2001), 145–159.

[Chow 49] W.-L. Chow "On Compact Complex Analytic Varieties." *Amer. J. Math.* 71 (1949), 893–914.

[Desboves 86] A. Desboves. "Résolution en nombres entiers et sous sa forme la plus générale de l'équation cubique, homegène à trois inconnues." *Nouv. Ann. de la Math. Ser. III* 5 (1886), 545–579.

[Fakhruddin 03] N. Fakhruddin. "Questions on Self Maps of Algebraic Varieties." *J. Ramanujan Math. Soc.* 18:2 (2003), 109–122.

[Fornæss 96] J. E. Fornæss. *Dynamics in Several Complex Variables*, CBMS Regional Conference Series in Mathematics, 87. Providence, RI: Amer. Math. Soc., 1996.

[Fornæss and Sibony 94] J. E. Fornæss and N. Sibony. "Complex Dynamics in Higher Dimension I." *Astérisque* 222 (1994), 201–231.

[Fornæss and Sibony 95a] J. E. Fornæss and N. Sibony. "Classification of Recurrent Domains for Some Holomorphic Maps." *Math. Ann.* 301:4 (1995), 813–820.

[Fornæss and Sibony 95b] J. E. Fornæss and N. Sibony. "Complex Dynamics in Higher Dimension II." In *Modern Methods in Complex Analysis*, edited by T. Bloom, D. Catlin, J. P. D'Angelo, and Y.-T. Siu, pp. 135–182, Ann. of Math. Stud., 137. Princeton, NJ: Princeton University Press, 1995.

[Fornæss and Sibony 95c] J. E. Fornæss and N. Sibony. "Oka's Inequality for Currents and Applications." *Math. Ann.* 301:3 (1995), 399–419.

[Fornæss and Sibony 01] J. E. Fornæss and N. Sibony. "Dynamics of $\mathbb{P}^2$ (Examples)." In *Laminations and Foliations in Dynamics, Geometry and Topology*, pp. 47–85, Contemp. Math. 269. Providence, RI: Amer. Math. Soc., 2001.

[Fornæss and Weickert 99] J. E. Fornæss and B. Weickert. "Attractors in $\mathbb{P}^2$." In *Several Complex Variables*, pp. 297–307, Math. Sci. Res. Inst. Publ. 37. Cambridge, UK: Cambridge Univ. Press, 1999.

[Ghys 84] É. Ghys. "Transformations holomorphes au voisinage d'une courbe de Jordan" *C. R. Acad. Sci. Paris Sér. I Math.* 298 (1984), 385–388.

[Gorodetski and Ilashenko 96] A. Gorodetski and Y. Ilyashenko. "Minimal and Strange Attractors." *Int. J. Bifurcations and Chaos* 6 (1996), 1177–1183.

[Griffiths and Harris 94] P. Griffiths and H. Harris. *Principles of Algebraic Geometry*. New York: Wiley, 1994.

[Guedj 05] V. Guedj. "Ergodic Properties of Rational Mappings with Large Topological Degree." *Ann. of Math.* 161 (2005), 1589–1607.

[Hesse 44] O. Hesse. "Über die Elimination der Variabeln aus drei algebraischen Gleichungen vom zweiten Grade mit zwei Variabeln." *Crelle's J.* 28 (1844), 68–96.

[Hubbard and Papadopol 94] J. H. Hubbard and P. Papadopol. "Superattractive Fixed Points in $\mathbb{C}^n$." *Indiana Univ. Math. J.* 43:1 (1994), 321–365.

[Jonsson and Weickert 00] M. Jonsson and B. Weickert. "A Nonalgebraic Attractor in $\mathbb{P}^2$." *Proc. Amer. Math. Soc.* 128:10 (2000), 2999–3002.

[Kan 94] I. Kan. "Open Sets of Diffeomorphisms Having Two Attractors, Each with an Everywhere Dense Basin." *Bull. Amer. Math. Soc.* 31 (1994), 68–74.

[Kaneko 02] K. Kaneko. "Dominance of Milnor Attractors in Globally Coupled Dynamical Systems with More Than 7 ± 2 Degrees of Freedom." *Phys. Rev. E.* 66 (2002), 055201.

[Kaneko 03] "Prevalence of Milnor Attractors and Chaotic Itinerancy in 'High'-Dimensional Dynamical Systems." In *Synchronization: Theory and Application,*, pp. 65–77, NATO Sci. Ser. II Math. Phys. Chem., 109. Dordrecht, The Netherlands: Kluwer Acad. Publ., 2003.

[Krushkal′ 79] S. L. Krushkal′. *Quasiconformal Mappings and Riemann Surfaces*. New York: John Wiley and Sons, 1979.

[Maistrenko et al. 98] Y. Maistrenko, V. Maistrenko, and A. Popovich. "Transverse Instability and Riddled Basins in a System of Two Coupled Logistic Maps." *Phys. Rev. E* 57 (1998), 2713–2724.

[de Melo and van Strien 93] W. de Melo and S. van Strien. *One-Dimensional Dynamics*. New York: Springer-Verlag, 1993.

[Milnor 85] J. Milnor. "On the Concept of Attractor." *Comm. Math. Phys.* 99 (1985), 177–195; "Correction and Remarks." *Comm. Math. Phys.* 102, 517–519.

[Milnor 06a] J. Milnor. "On Lattès Maps." In *Dynamics on the Riemann Sphere*, A Bodil Branner Festschrift, edited by P. Hjorth and C. L. Petersen. European Math. Soc., 2006.

[Milnor 06b] J. Milnor. *Dynamics in One Complex Variable*, Annals of Math. Study 130. Princeton, NJ: Princeton University Press, 2006.

[Ott et al. 93] E. Ott, J. Sommerer, J. Alexander, I. Kan, and J. Yorke. "Scaling Behavior of Chaotic Systems with Riddled Basins." *Phys. Rev. Lett.* 71 (1993), 4134–4137.

[Ott and Sommerer 94] E. Ott and J. Sommerer. "Blowout Bifurcations: The Occurrence of Riddled Basins and On-Off Indeterminacy." *Phys. Lett. A* 188 (1994), 39–47.

[Platt et al. 93] N. Platt, E. Spiegel, and C. Tresser. "On-Off Intermittency: A Mechanism for Bursting." *Phys. Rev. Lett.* 70 (1993), 279–282.

[Shishikura 87] M. Shishikura. "On the Quasiconformal Surgery of Rational Functions." *Ann. Sci. École Norm. Sup.(4)*20:1 (1987), 1–29.

[Sibony 99] N. Sibony. "Dynamique des applications rationnelles de $\mathbb{P}^k$." *Dynamique et Geometrie Complexes, Panoramas et Syntheses* 8 (1999), 97–185.

[Ueda 93] T. Ueda. "Complex Dynamical Systems on Projective Spaces." In *Chaotic Dynamical Systems*, pp. 120–138. River Edge, NJ: World Scientif. Publ., 1993.

[Yoccoz 02] J.-C. Yoccoz. "Analytic Linearization of Circle Diffeomorphisms." In *Dynamical Systems and Small Divisors (Cetraro, 1998)*, pp. 125–173, Lecture Notes in Math. 1784. Berlin: Springer, 2002.

Araceli Bonifant, Mathematics Department, University of Rhode Island, 9 Greenhouse Road, Suite 3, Kingston, RI 02881-0816 (bonifant@math.uri.edu)

John Milnor, Institute for Mathematical Sciences, Stony Brook University, Stony Brook, NY. 11794-3660 (jack@math.sunysb.edu)

Received January 1, 2006; accepted October 31, 2006.